ORNL/ATD--70

DE93 011459

THERMOGRAPHIC PROPERTIES OF EIGHT BLUE-EMITTING PHOSPHORS

D. M. Cunningham
S. W. Allison
D. B. Smith

Date Published-January 1993

Prepared by the
Engineering Technology Division
of the
Oak Ridge National Laboratory
Oak Ridge, Tennessee 37831-7280
managed by
MARTIN MARIETTA ENERGY SYSTEMS, INC.
for the
U. S. DEPARTMENT OF ENERGY
under contract DE-AC05-84OR21400

CONTENTS

CONTENTS (Continued)

LIST OF FIGURES

LIST OF TABLES

ABSTRACT

We examined the effect of temperature on the light emission and absorption properties of eight phosphorescent compounds. The phosphors are commercially produced powders that emit mainly in the blue region when illuminated with ultraviolet light (220 to 400 nm). Excitation and emission spectra taken over the temperature range of 20°C to 350°C are presented for these phosphors. Data from the spectra indicate a strong temperature dependence over this temperature range. Maximum relative intensity changed as a function of temperature in every phosphor examined. In some samples, spectral band shifts and bandwidths also changed with temperature. Of these phosphors, $BaMg_2Al_{16}O_{27}$:Eu and $Ba_3(PO_4)_2$:Eu are candidates for higher-temperature studies.

1. INTRODUCTION

Phosphor thermometry offers unique advantages for temperature measurement, including the ability to record temperatures ranging from near 0 K to 1800 K. This can only be possible with a combination of phosphors where each covers a portion of this range. For effectual measurement, the temperature-dependent characteristics of the different phosphor emissions must be distinct from one another. Many other applications of phosphor thermometry also require specific properties of the phosphor (according to environment, temperature range, etc.). Thus, a pool of knowledge characterizing specific thermographic properties of phosphors is valuable.

This experiment examined the thermographic properties of eight blue-emitting phosphors at temperatures ranging from 20°C (room temperature) to 350°C. All eight phosphors exhibited strong temperature dependence in this range.

2. BACKGROUND

Phosphors are crystalline compounds with a low concentration of dopant ions. In a crystal lattice, there is generally a positive cation and a negative anion. The dopant ion takes the place of the cation in a small percentage of the basis cells. For example, in the phosphor $Ba_3(PO_4)_2$:Eu, barium is a divalent cation while the phosphate is negatively trivalent. In this case, europium is a positive divalent ion replacing the barium ion. Dopant ions (activators) are rare-earth, transition, or metal elements and produce the fluorescence. Interaction between the crystal host, $Ba_3(PO_4)_2$, and the dopant ion, Eu, largely determines the temperature-dependent characteristics of the phosphor.

To understand phosphor emissions and their thermographic properties, we must study the doped crystal. The dopant ion has valence electrons at some ground state. Empty shells, which are characteristic of the dopant ion, exist at distinct energy levels above the ground state [see Fig. 1(a)]. For some phosphors, a charge transfer state (CTS) intersects these higher energy levels. The CTS represents the average energy required for a ground-state electron to interact with the crystal host and corresponds to the distance of the activator ion to its nearest neighbor.

Free electrons in the dopant ion can be excited by three mechanisms: (1) by direct excitation, (2) by CTS excitation, and (3) by vibrational energy transmitted through the host lattice. Direct excitation occurs when an electron in a valence state absorbs a photon with the energy required to cause a transition to a higher energy level. The electron makes the transition to its excited state and enters into some vibrational level within this state. In Fig. 1(a) this corresponds to movement along the energy-level curve between A and B. These vibrations are damped, leaving the system at equilibrium. The electron will then emit a photon and return to its ground state. There is also a possibility that the electron will, when initially excited, vibrate between A' and B', as shown in Fig 1(a). This vibrational level intersects the CTS. In this case, the electron can make another transition to the CTS. When relaxing from the CTS, the electron may go directly back to its ground state without producing radiation. The electron may also return to another high-energy state within the dopant ion (provided it is lower than the one it was previously occupying) and then proceed to

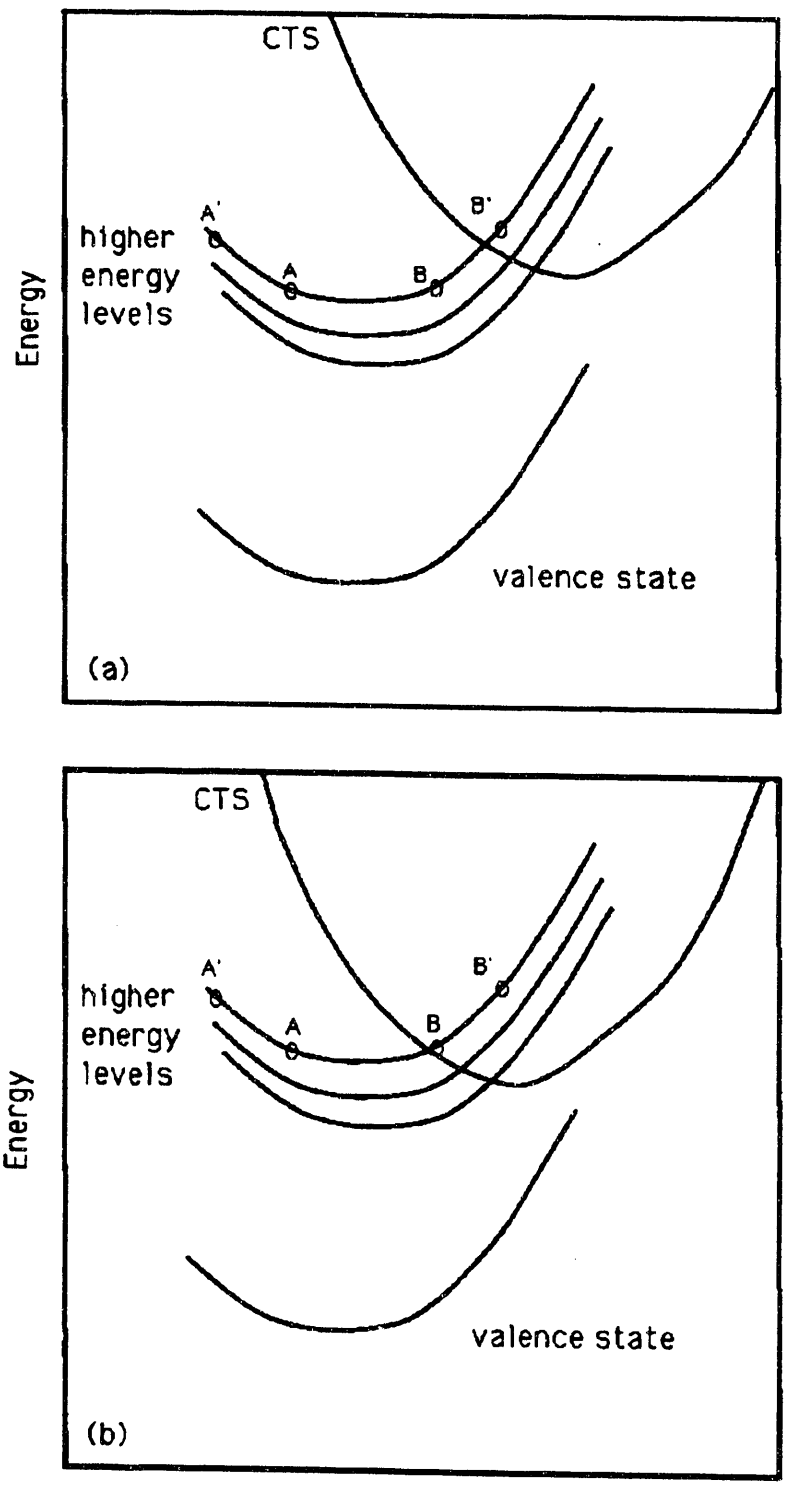

Fig. 1. Configuration coordinate model. (a) shows possible transitions, (b) shows the effect temperature has on the model. Note that the CTS band has shifted in position.

the ground state. The radiative energy from this transition is equal to the energy difference between the corresponding energy levels.

Charge transfer state excitation occurs when an electron at ground state is excited by a photon with enough energy to cause a transition directly to the charge transfer band. The energy required to make this transition increases as the distance between the crystal host and the dopant ion increases. When the electron eventually returns to its ground state, it can take several paths. If it returns directly to the ground state, all energy loss is nonradiative. The electron may also travel to other energy states below the CTS. These states correspond to energy levels characteristic of the dopant ion. When this occurs, a nonradiative transition takes place between the CTS and lower-energy levels. A radiative transition can then occur between this new energy state and the ground state.

Ground-state electrons can also be excited by vibrational energy transferred through the crystal lattice. The vibrational energy is quantized in energy units called phonons. Phonons can be transmitted from an excited electron to one in a valence state. Radiative and nonradiative transitions can occur as previously described with this vibrational excitation.

Increase or decrease in temperature affects the vibrations of the crystal lattice. In the case of a temperature increase, vibrations within the crystal also increase. This changes the average distance of the dopant ion from the nearest-neighbor ion, thus changing the configuration coordinate diagram [see Fig. 1(b)]. Note that the position of the charge transfer band has shifted, significantly lowering the required vibrational level for a CTS transition. This increases the probability that an excited electron will enter the charge transfer band. As a result, characteristics such as emission intensity, bandwidth, and band position will be altered.

3. EXPERIMENTAL APPARATUS

A Perkin-Elmer 650-10S Spectrophotometer (Fig. 2) was used to obtain emission and excitation spectra from the phosphor samples. A xenon lamp was the excitation light source. Light traveling from the lamp hit a diffraction grating which selected a narrow band of light to excite the phosphor. The grating angle could be adjusted to vary the wavelength of excitation light. The excitation light passed through slit 1 (S1) and illuminated the phosphor sample. The sample then emitted radiation through slit 2 (S2) and continued to a diffraction grating. The grating (adjustable) selected a narrow band of emitted light to continue to the photomultiplier tube (PMT). The PMT produced an output voltage corresponding to the intensity of the isolated emission radiation. The amplified PMT signal was sent to a chart recorder that produced a plot of relative emission intensity vs wavelength (of either emission or excitation light). Wavelength was determined by the rate at which the diffraction grating rotates. The plots were digitized and rescaled with SigmaScan™ and SigmaPlot™, respectively.

ORNL-DWG 92-12941

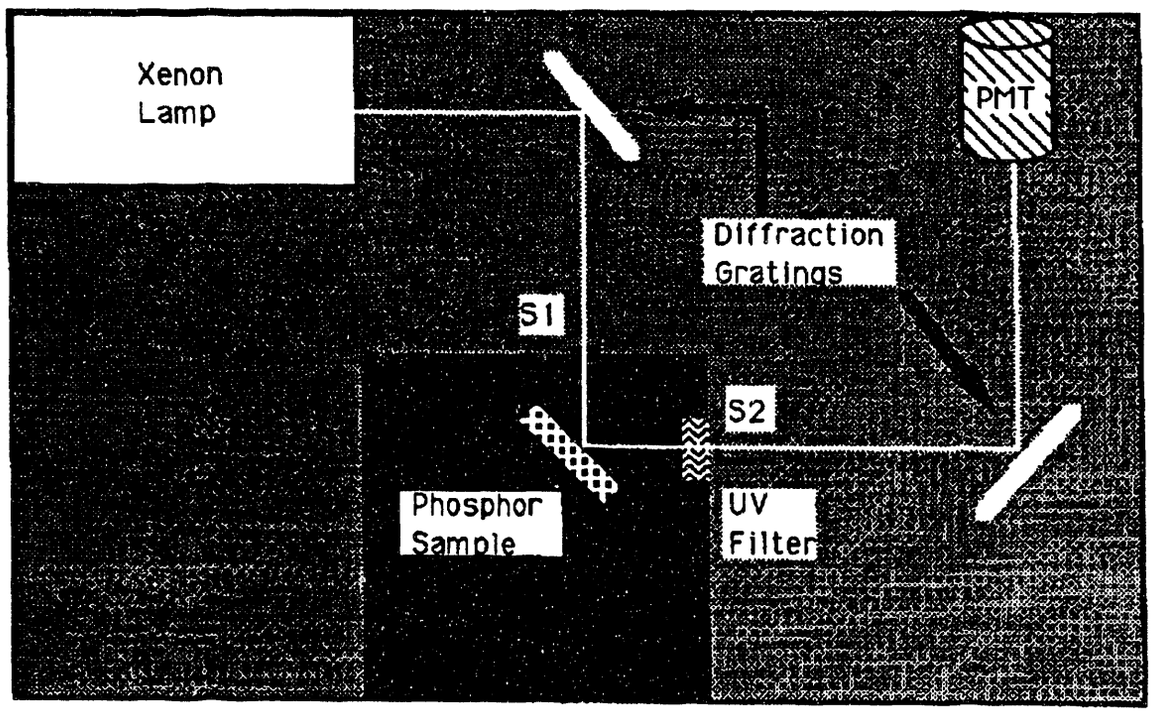

Fig. 2. Spectrophotometer layout.

To compensate for variations in intensity from the xenon lamp, a portion of the excitation beam is diverted to a monitor detector. This allows the spectrophotometer to adjust the output from the photomultiplier, ensuring the ratio of the excitation and emission signals remains the same.

The width of slits for S1 and S2 can be adjusted. For this experiment, the width of both slits remained constant at 2 nm. The slit sizes were equal to prevent any possibility of detector saturation (when high light levels are used). However, the small slit width also results in a high signal-to-noise ratio. Since this experiment is primarily comparative, this was determined to be of minimal importance.

The temperature of the phosphor sample was regulated by a small oven (see Fig. 3) constructed to be contained within the housing of the spectrophotometer. Light entering S1 continues directly through a quartz optical port and illuminates the sample. Likewise, emission light could exit through a second optical port and S2. A thermocouple positioned approximately 2 mm from the sample was used to measure the temperature of the phosphor. The oven temperature was controlled manually by a variable ac power supply. Because no regulator was present, the operator was required to monitor the thermocouple to adjust and maintain steady temperatures inside the oven.

A uv filter, which blocked light below 400 nm, was placed in front of S2. Emission spectra for this experiment were recorded within the range of 400 to 700 nm. Excitation light (generally between 220 to 400 nm) could also pass through S2. Although the excitation wavelengths themselves posed no threat to emission detection (because emission wavelengths detected were significantly longer), the second-order lines from excitation light did pose a problem. The uv filter chosen allows light of 400 nm and longer to pass through S2. Second-order lines of 800 nm and above can also continue to the diffraction grating. However, the filter neither affects the range of emission light we wished to detect (400 to 700 nm), nor allows misleading second-order excitation lines to appear in spectra for the range we wished to study.

4. RESULTS

The data and discussion of results will be presented separately for each phosphor. To avoid repetition, relevant information describing how data were obtained and analyzed will be presented here.

Emission spectra were taken by scanning the wavelengths of emitted light from the sample at a constant excitation wavelength. Conversely, the excitation spectra were varied by scanning the excitation light while keeping detection of the emission light wavelength constant. The constant excitation and emission wavelengths were determined by finding the maximum relative intensity that could be obtained at ambient temperature (i.e., the emission and excitation spectra should have the same maxima at room temperature).

For each phosphor sample, three separate sets of emission and excitation spectra were taken at several temperatures over the range of 20°C to 350°C. This was done to demonstrate the reproducibility of data and to identify temperature-dependent trends. Run 1 was a preliminary run to determine the basic thermographic characteristics of the phosphor. Care was taken to achieve a

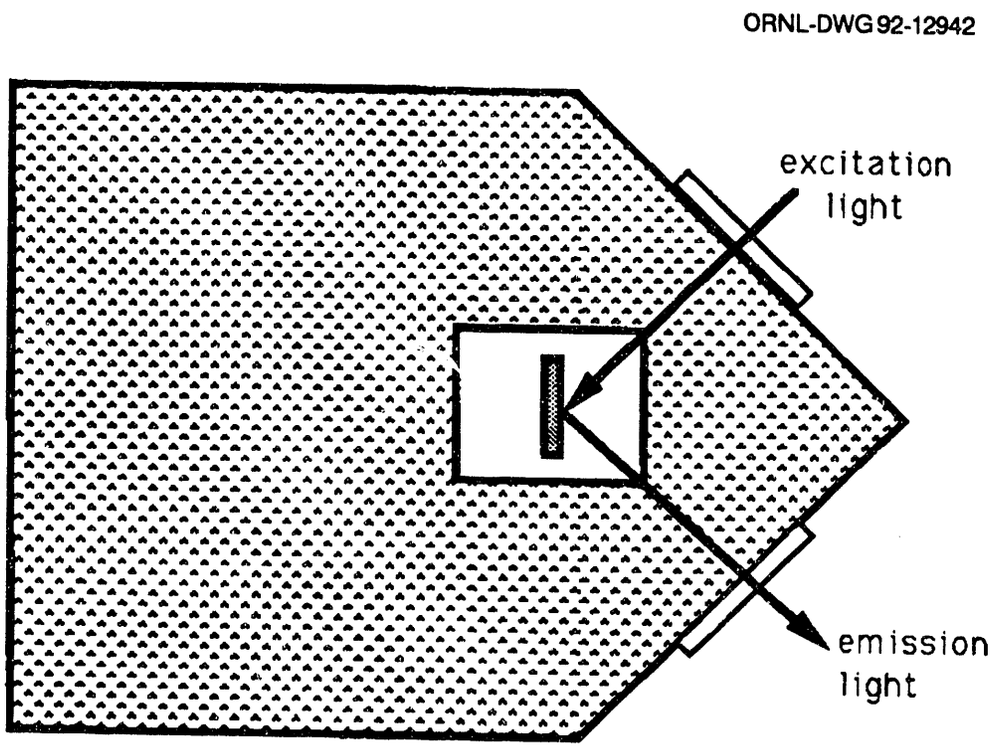

Fig. 3. Oven, top view.

high relative emission intensity at room temperature to ensure the best possible readings at higher temperatures (where intensities are generally significantly lower). Runs 2 and 3 were taken consecutively to better show reproducibility. For simplicity, only emission and excitation spectra for one data set (Run 2) are presented to show the general trend of the entire body of data. All data sets are represented in plots directly showing temperature-dependent relationships and the equations empirically found (unless otherwise stated).

Emission intensities could only be measured in relative units. To avoid misinterpretation of these relative units, intensity was normalized relative to the maximum intensity for Run 2 at ambient temperature for each phosphor. Percentage decrease in relative intensity is also more obvious with normalized data.

Bandwidth for the spectra is the full width of the spectral band at half maximum intensity. The maxima were measured from each plot. At half this height, the bandwidth was measured.

Equations characterizing temperature dependence were found using numerical methods. A least-squares procedure was used to fit empirical formulas to the data.

4.1 $BaMg_2Al_{16}O_{27}$:Eu (Sylvania Type 2461)

4.1.1 Emission

Excitation light at 380 nm produced emission spectra shown in Fig. 4(a). The collection of spectra shows a large decrease in maximum relative intensity from room temperature to 50°C. Temperatures above 50°C produce uniformly decreasing intensities. No drastic change in band position appears in the emission spectra.

Comparing temperature-dependent data for relative intensity from all three data sets reveals two distinct trends [Fig. 4(b)]. Run 1 indicates an increase in intensity from ambient to 150°C. A sharp linear decrease occurs at temperatures higher than 150°C. A linear fit to these data gives

$$I_{max} = -6.701\text{x}10^{-3} \cdot T + 3.561 , \quad (1)$$

where I_{max} is the maximum relative intensity and T is the temperature. This implies I_{max} decreases 0.0067 unit for every 1°C increase. From the I_{max}-axis intercept, one can ascertain that the intensities in Run 1 are approximately 3.5 times larger than those in Runs 2 and 3. Intensities from Runs 2 and 3 have similar trends and appear to fit to the equation

$$I_{max} = -2.026\text{x}10^{-3} \cdot T + 0.8566 . \quad (2)$$

Again, this indicates a 0.002 unit (or 0.2%) decrease for every 1°C increase.

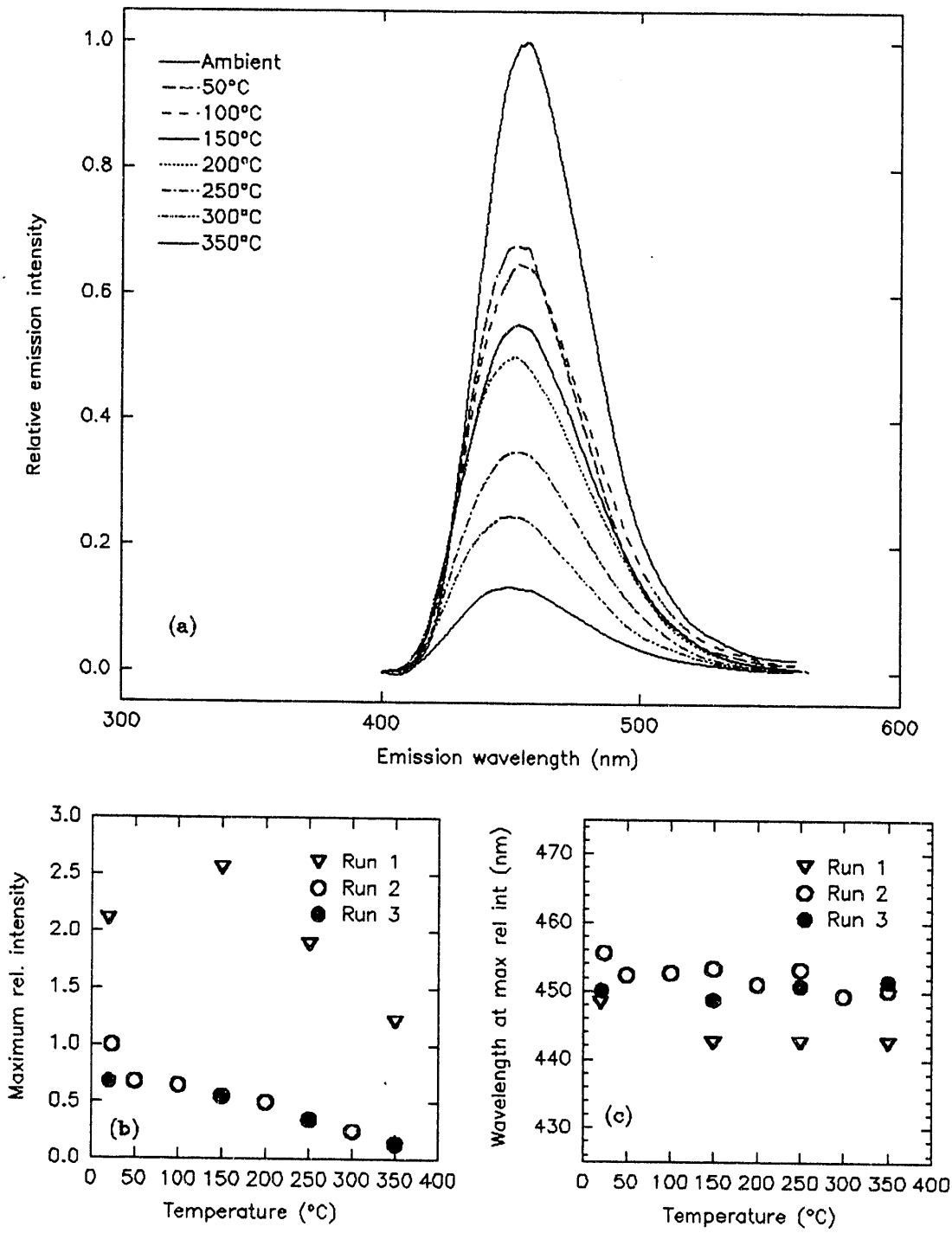

Fig. 4. Emission data for $BaMg_2Al_{16}O_{27}$:Eu. (a) Emission spectra, (b) maximum relative intensity vs temperature, (c) band position vs temperature.

Band shift was found to have no temperature dependence. Figure 4(c) illustrates this with a constant band position at about 450 nm over the entire temperature range. It is interesting to note that data from Run 1 maintain a band position at slightly shorter wavelengths than Runs 2 and 3.

Results regarding bandwidth trends conflict (see Table 1). Run 1 implies no temperature dependence is present with a constant width at 55.9 nm. Runs 2 and 3 indicate a slight increase of 6.5 nm in bandwidth through the entire temperature range. Because this change is so small, it can be considered insignificant; however, the trend should be noted. The difference in bandwidth between data sets (up to 15 nm) cannot be explained.

Table 1. Bandwidth of $BaMg_2Al_{16}O_{27}$:Eu emission as a function of temperature

	Bandwidth (nm)		
T(°C)	Run 1	Run 2	Run 3
amb	55.9	41	41
50	-	42.8	-
100	-	42.8	-
150	55.9	42.8	45.2
200	-	43.7	-
250	55.9	45.2	46.3
300	-	45.2	-
350	55.9		47.5

4.1.2 Excitation

Excitation spectra depicted in Fig. 5(a) were obtained for emissions of 450 nm. The spectra show a sharp decrease in maximum relative intensity from ambient to 50°C and continue to drop in a more gradual, uniform fashion through 350°C. A band shift does not appear in this spectra set.

Intensities show trends similar to those of the emission spectra [Fig. 5(b)]. In Run 1, intensities increase through 150°C and then decrease sharply. In Runs 2 and 3, the intensities decrease at a more gradual rate (a 14% drop from the original intensity per 100°C) when compared to Run 1. The equation describing temperature-dependent behavior from Runs 2 and 3 is

$$I_{max} = -1.43\text{x}10^{-3} \cdot T + 0.7794 \, . \qquad (3)$$

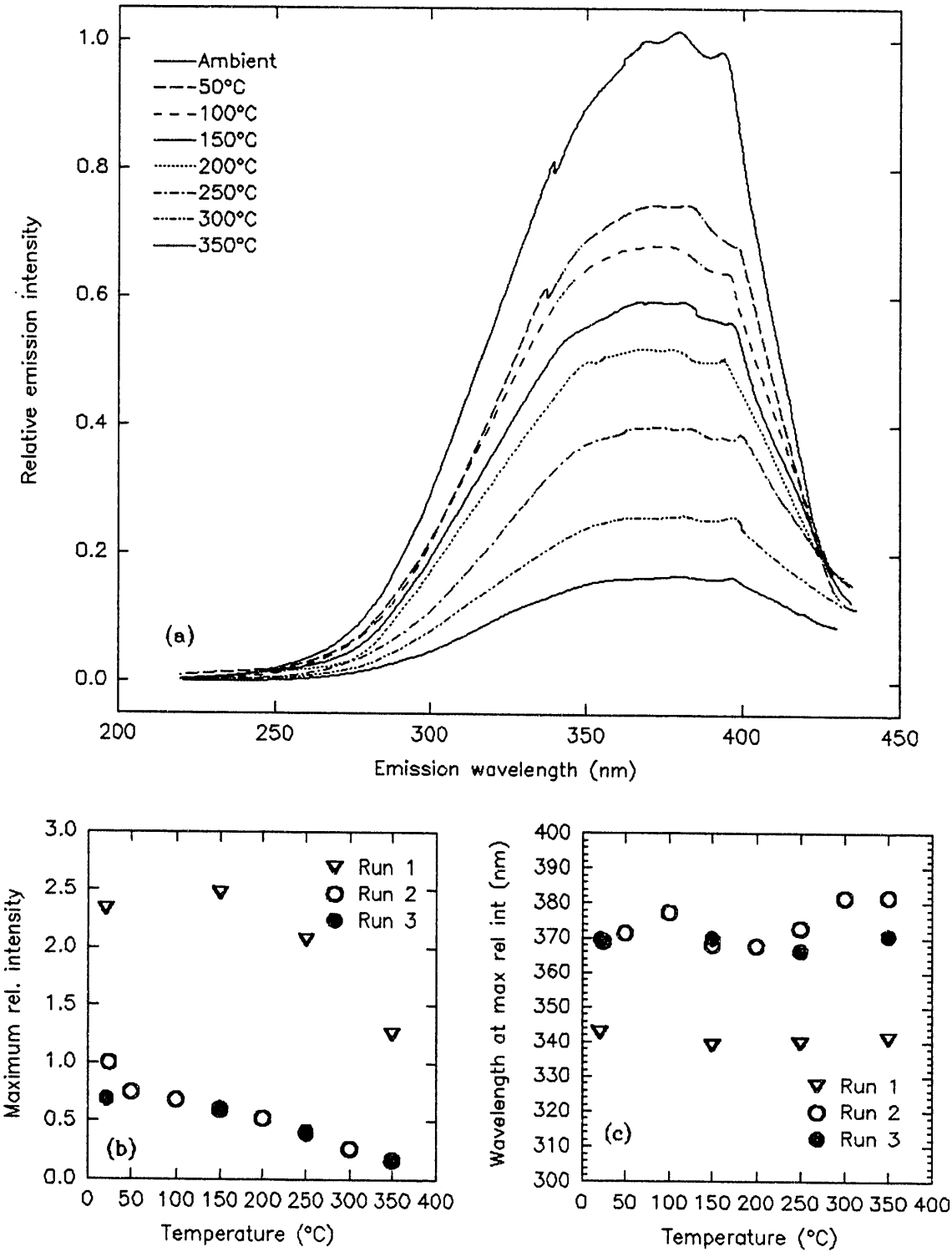

Fig. 5. Excitation data for $BaMg_2Al_{16}O_{27}$:Eu. (a) Excitation spectra, (b) maximum relative intensity vs temperature, (c) band position vs temperature.

Run 1 also indicates a temperature-dependent decrease in intensity but fits the equation

$$I_{max} = -6.08\text{x}10^{-3} \cdot T + 3.451 \, . \qquad (4)$$

No band shift is evident with varying temperature. Fig. 5(c) shows data to be constant at 340 and 370 nm. Once again, Run 1 deviates from Runs 2 and 3 but supports the trend of a constant band position through the temperature range studied.

No temperature-dependent trend for bandwidth is evident (see Table 2). Run 2 shows sporadic jumps in bandwidth, whereas Runs 1 and 3 show broadening. Run 1 excitation spectra are also significantly broader. With the present data, it is difficult to determine if any trend exists.

Table 2. Bandwidth of $BaMg_2Al_{16}O_{27}$:Eu excitation as a function of temperature

	Bandwidth (nm)		
T(°C)	Run 1	Run 2	Run 3
amb	111	94.9	97.4
50	-	100	-
100	-	97.4	
150	1169	105.1	100
200	-	102.5	-
250	120	97.4	110.2

The most promising temperature-dependent property for this sample exists in the decrease of maximum relative intensity. It decreases linearly as temperature increases from 150°C to 350°C. Run 1 also indicates that this phosphor may have useful thermographic characteristics for temperatures higher than 350°C. This is not easily seen on the relative intensity scale chosen for data evaluation. Raw data indicate that the unnormalized relative intensity at 350°C is very high (in other words, the PMT received a higher intensity of light for this sample than others at 350°C). Figure 4(a) indicates that quenching of the phosphor has not occurred at 350°C. This leaves the possibility for study in higher-temperature regions.

4.2 $Ca_5F(PO_4)_3$:Sb (Sylvania Type 2440)

4.2.1 Emission

Excitation light at 280 nm was used to create emission spectra for this phosphor. Although there is a slight increase in maxima from ambient to 50°C, the relative intensity decreases overall as temperature increases [Fig. 6(a)]. Spectra also suggest a rapid reduction in intensity maxima over the range 150°C to 250°C.

The temperature-dependent relationship is shown in Fig. 6(b). The data indicate a rapid decrease in intensity at the middle of the temperature range studied with more subtle decreases at the ends of the range. A decrease of 77.8% occurs throughout the range.

A slight spectral shift can be seen in emission spectra. Figure 6(c) indicates a shift toward shorter wavelengths occurs in lower temperatures. This trend then stabilizes, centering maxima around 450 nm for temperatures greater than 120°C.

Bandwidth appears to have no temperature dependence. Table 3 lists bandwidths for all three data sets. Run 1 maintains a width of approximately 96 nm. Run 2 spectra appear a bit more narrow at 92 nm and Run 3 spectra are approximately 98 nm. Although each spectra set produces bands with slightly different widths, no consistent change occurs with varied temperature.

Table 3. Bandwidth of $Ca_5F(PO_4)_3$:Sb emission as a function of temperature

	Bandwidth (nm)		
T(°C)	Run 1	Run 2	Run 3
amb	96	95.4	98.7
50	-	98.7	-
100	-	92.1	-
150	96	92.1	95.4
200	-	92.1	-
250	91.7	98.1	98.7

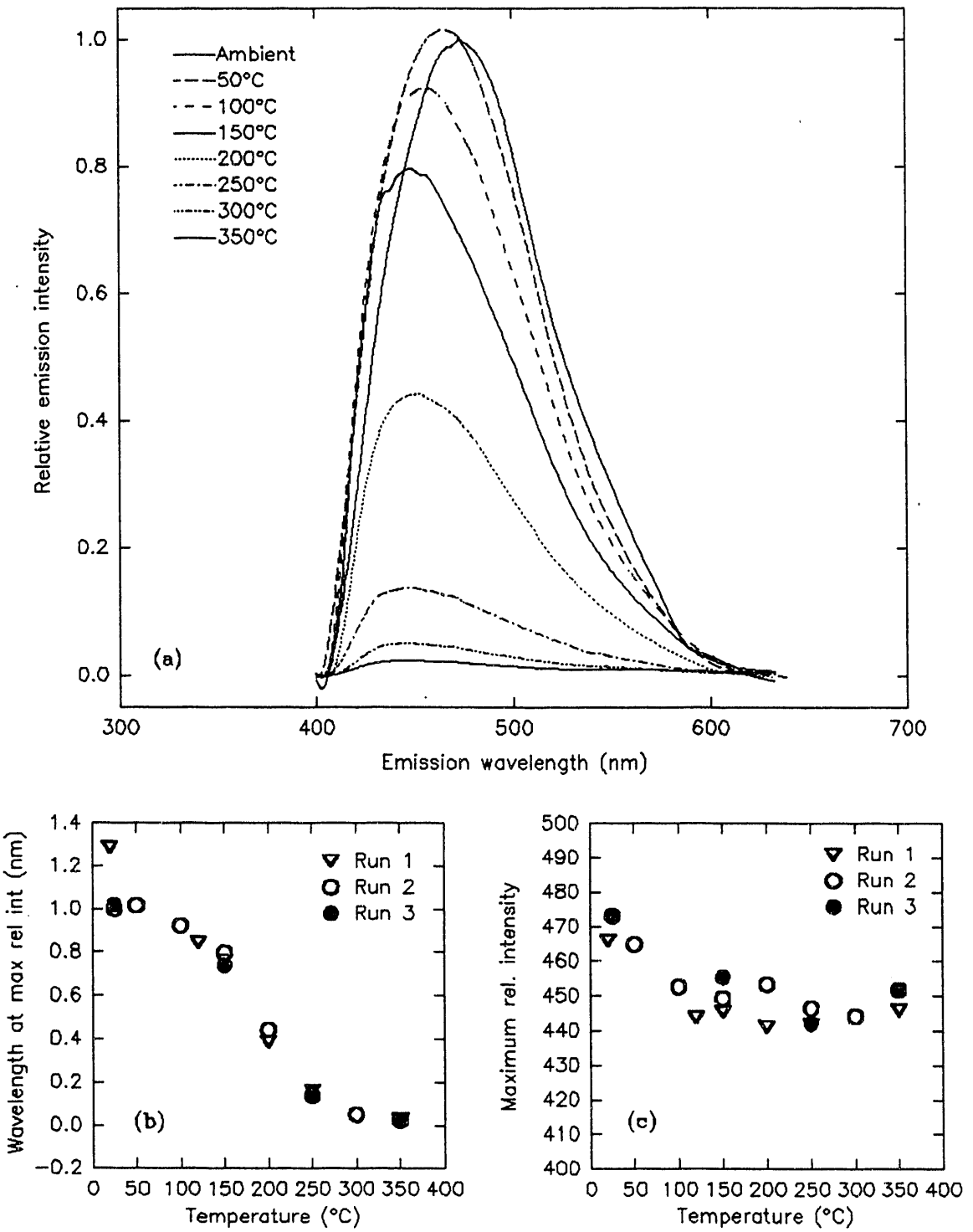

Fig. 6. Emission data for $Ca_5F(PO_4)_3$:Sb. (a) Emission spectra, (b) maximum relative intensity vs temperature, (c) band position vs temperature.

4.2.2 Excitation

Excitation spectra were found for emissions of 470-nm light. Figures 7(a) and 7(b) are similar to those of the emission spectra, in that they show a rapid decrease in intensity at midrange with a slight decrease at low and high ends of the range. The percent reduction throughout the range is nearly identical but slightly higher than that of the emission spectra at 78.8%.

Figure 7(c) shows no clear relationship for spectral shift in excitation spectra. The sporadic distribution of data is inconclusive.

Broadening of bandwidth in excitation spectra appears to have temperature dependence. Table 4 shows a marked and consistent broadening of bandwidth from about 48 nm to 63 nm for Runs 2 and 3. Run 1 shows the same increase with conflicting data for the final two points. Despite these conflicting data, temperature dependence is probable.

The most interesting and obviously temperature-dependent characteristic of this sample is maximum relative intensity. The range (100°C to 250°C) in which the sharp decrease in maxima occurs provides a very sensitive range for temperature readings. Emission spectra show a small shift toward higher frequencies as temperatures are elevated to 150°C. This shift is not large enough for use in temperature measurement, but may be significant in applications using more than one phosphor (because the emission peaks of different phosphors might overlap).

Table 4. Bandwidth of $Ca_5F(PO_4)_3$:Sb excitation as a function of temperature

	Bandwidth (nm)		
T(°C)	Run 1	Run 2	Run 3
amb	48	47.7	49.4
50	-	49.4	-
100	-	51	-
150	56	57.6	55.9
200	-	59.2	-
250	52	62.5	62.5

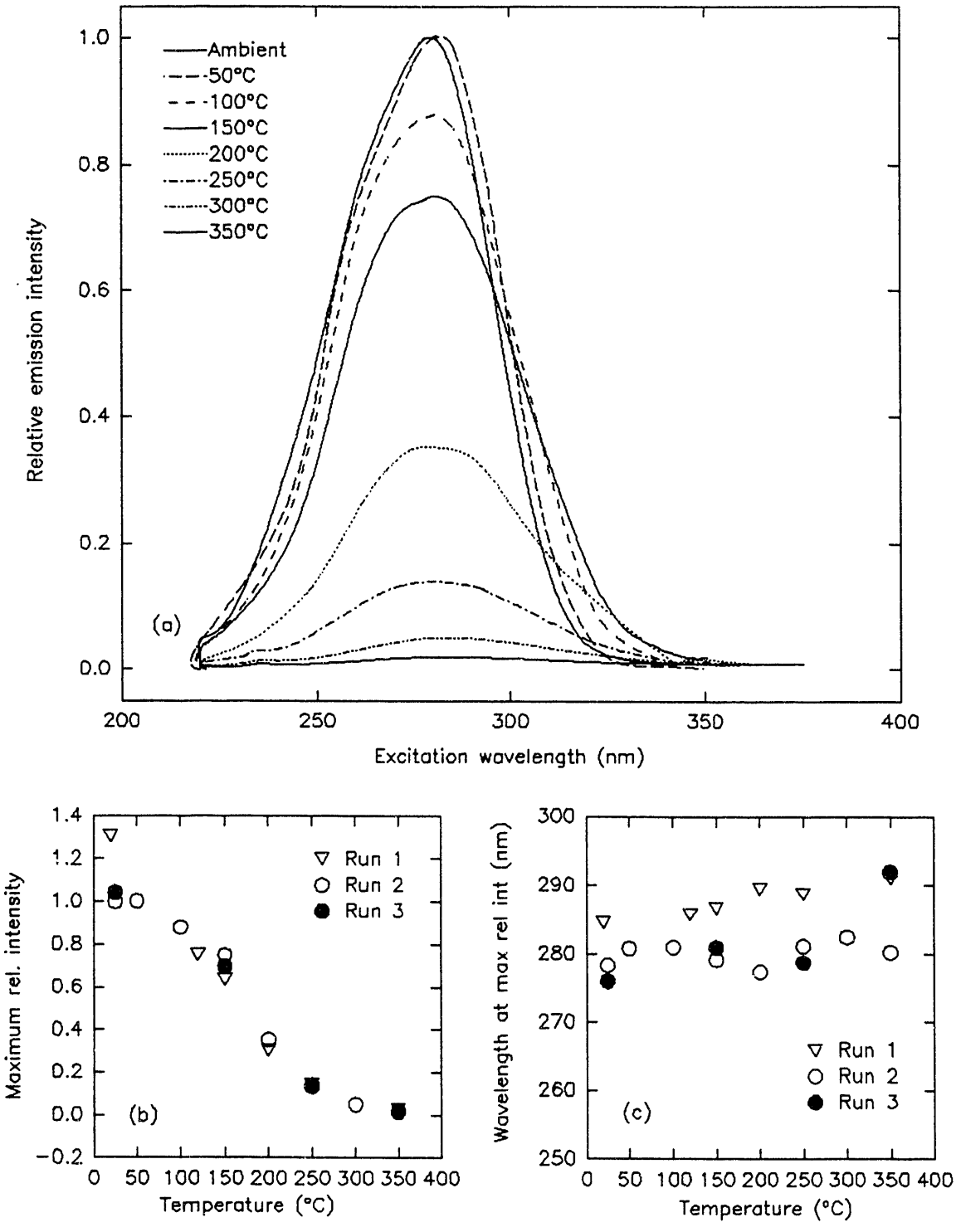

Fig. 7. Excitation data for $Ca_5F(PO_4)_3$:Sb. (a) Excitation spectra, (b) maximum relative intensity vs temperature, (c) band position vs temperature.

4.3 $Sr_5Cl(PO_4)_3$:Eu (Sylvania Type 247)

4.3.1 Emission

Light of 396-nm wavelength was used to excite this phosphor creating spectra in Fig. 8(a). These spectra exhibit a strong, regular decrease in maximum relative intensity as temperature increases. This is illustrated more clearly in Fig. 8(b). The linear relationship between the relative intensities and temperature can be described by the equation

$$I_{max} = -3.231\text{x}10^{-3} \cdot T + 1.163 \, . \tag{5}$$

This translates to approximately a 32% linear decrease from the intensity at ambient for every 100°C increase.

The band shift exhibits no noticeable temperature dependence. In Fig. 8(c) it is clear that the wavelength at maximum intensity for emission spectra remains constant at approximately 449 nm.

Bandwidth broadens noticeably as temperature increases. Table 5 indicates that bands increase by 30 nm in width for emission spectra. The spectra suggest a rapid broadening over the entire temperature range.

Table 5. Bandwidth of $Sr_5Cl(PO_4)_3$:Eu emission as a function of temperature

	Bandwidth (nm)		
T(°C)	Run 1	Run 2	Run 3
amb	29.6	28.6	28.6
50	-	28.6	-
100	-	33.3	-
150	37	33.3	35.7
200	-	38.1	-
250	44.4	38.1	38.1
300	-	40.5	-
350	59.3	47.6	-

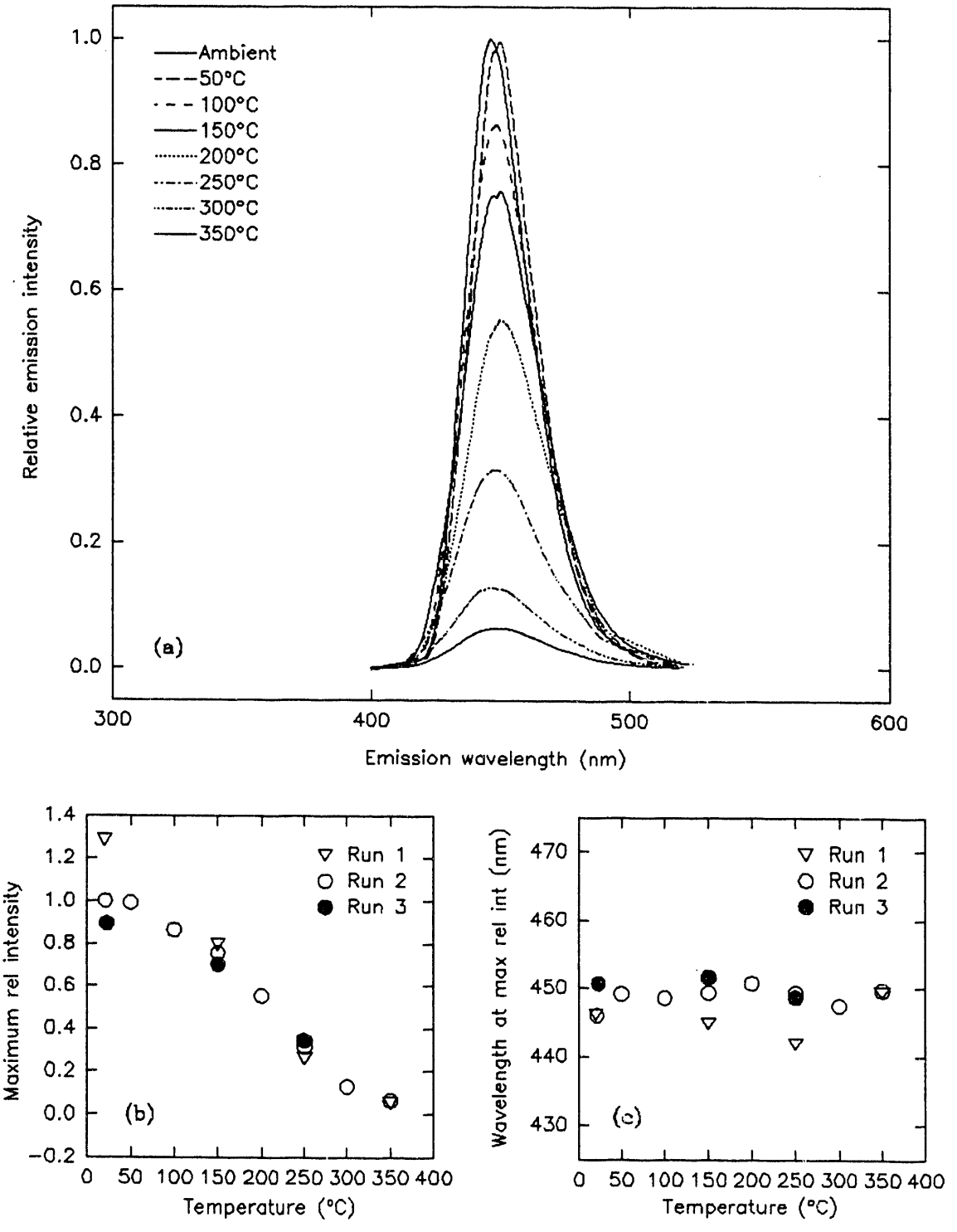

Fig. 8. Emission data for $Sr_5Cl(PO_4)_3$:Eu. (a) Emission spectra, (b) maximum relative intensity vs temperature.

4.3.2 Excitation

Spectra shown in Fig. 9(a) were found for emissions of 452 nm. Again, a very regular decrease in relative intensity is exhibited throughout the entire temperature range studied. The predictability of the data is obvious in Fig 9(b). Here, the plot of relative intensity against temperature yields a linear pattern. The decrease in intensity is nearly identical to emission spectra with a 31.6% decrease for every 100°C.

Excitation spectra show a little more variation in band position [Fig. 9(c)] than the emission spectra. However, the bands' maxima remain within about 7 nm of one another and show no decisive movement toward longer or shorter wavelengths. For these reasons, spectral shift is thought to have no temperature dependence.

There does appear to be a broadening in bandwidth which is related to temperature. Table 6 depicts an increase of 13 nm from room temperature to 250°C. Bandwidth for Run 1 is also noted to be considerably more narrow than for other data sets, but does have a similar gradual broadening trend.

Table 6. Bandwidth of $Sr_5Cl(PO_4)_3$:Eu excitation as a function of temperature

	Bandwidth (nm)		
T(°C)	Run 1	Run 2	Run 3
amb	126.9	167.5	170
50	-	170	-
100	-	-	-
150	130.8	167.5	-
200	-	175	-
250	134.6	180	172.5

Once again, maximum relative intensities are observed to exhibit strong temperature dependence. Broadening of the emission band also appears to be a strong thermographic property. This, combined with a constant spectral band position, provides favorable characteristics for thermometry applications.

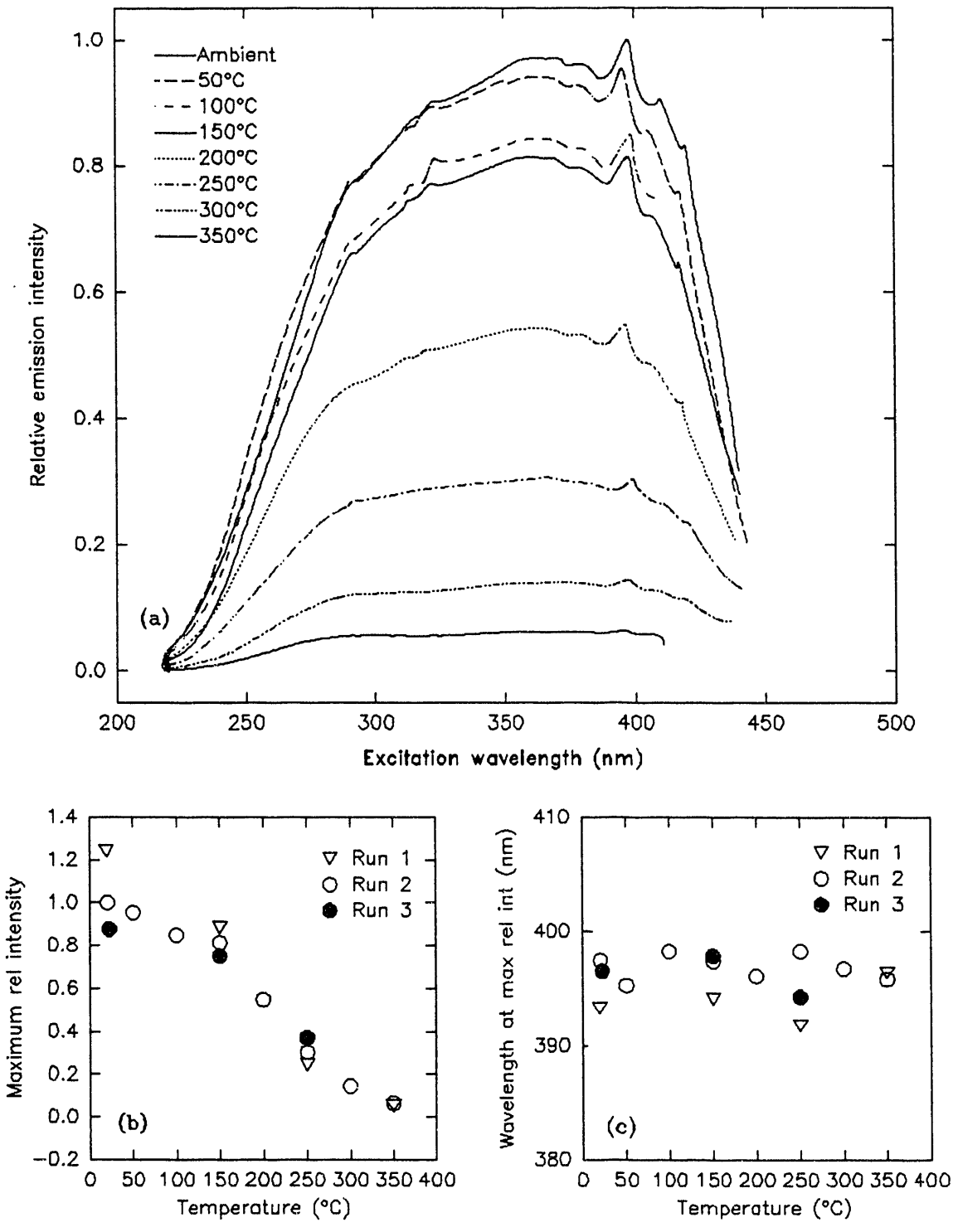

Fig. 9. Excitation data for $Sr_5Cl(PO_4)_3$:Eu. (a) Excitation spectra, (b) maximum relative intensity vs temperature, (c) band position vs temperature.

4.4 $Sr_2P_2O_7$:Sn (Sylvania Type 243)

4.4.1 Emission

When excited by 270-nm light, a decrease in relative intensity and band shift can be seen in emission spectra [Fig. 10(a)]. The decrease shows strong temperature dependence as seen in Fig. 10(b).

Temperatures above 150°C indicate a linear trend. Data from Run 1 creates a steeper slope and has an intensity value at 150°C, much larger than the other data sets. The rate relative intensity decreases over this range from data for Runs 2 and 3 can be written as

$$I_{max} = -2.023\text{x}10^{-3}\cdot T + 1.206 . \quad (6)$$

Run 1 decreases 33% for every 100°C increase. This is shown in the corresponding equation

$$I_{max} = -3.301\text{x}10^{-3}\cdot T + 1.697 . \quad (7)$$

Intensities for Runs 1 and 3 indicate an increase in value between ambient and 150°C, whereas Run 2 shows a decrease. This inconsistency may be due to the spectrophotometer, which will be discussed further in the Conclusion.

Band shift, which also was quite visually apparent in Fig. 10(a), can be seen more clearly when plotted against temperature. Fig. 10(c) shows a gradual, yet extremely consistent band shift toward shorter wavelengths as temperature was increased. The line best fit to the data is

$$I_{max} = -4.42\text{x}10^{-2}\cdot T + 452.6 . \quad (8)$$

This indicates that the emission spectral band shifts toward shorter wavelengths, 4.4 nm for every 100°C rise in temperature.

Bandwidths for emission spectra remain constant through 100°C. Temperatures above 100°C yield more narrow spectral bands (see Table 7) which decrease in width with increasing temperature.

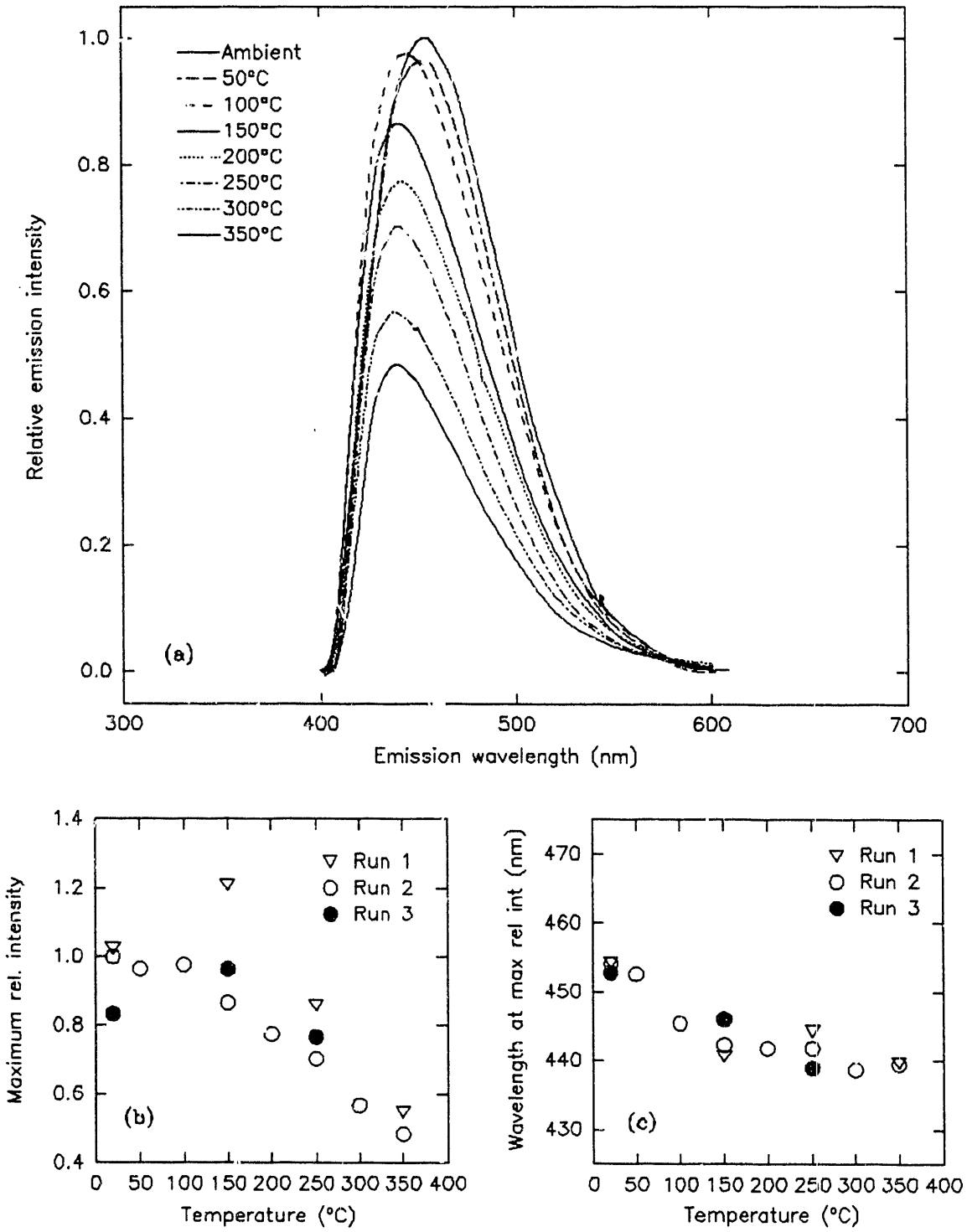

Fig. 10. Emission data for $Sr_2P_2O_7$:Sn. (a) Emission spectra, (b) maximum relative intensity vs temperature, (c) band position vs temperature.

Table 7. Bandwidth of $Sr_2P_2O_7$:Sn emission as function of temperature

	Bandwidth (nm)		
T(°C)	Run 1	Run 2	Run 3
amb	79	79	79
50	-	79	-
100	-	79	-
150	73.5	72.4	75.7
200	-	75.7	-
250	67.7	72.4	72.4
300	-	72.4	-
350	64.7	69.1	-

4.4.2 Excitation

Excitation spectra shown in Fig. 11(a) were obtained for emission of 442 nm. As with the emission spectra, excitation appears to exhibit a strong temperature dependence for both relative intensity and spectral band shift. Fig. 11(b) illustrates the temperature-dependent behavior. Temperature-dependent behavior adheres to trends found in the emission data. Run 1 decreases from its original intensity by 32.4% every 100°C elevation through the range 150°C to 350°C. Runs 2 and 3 decrease by only 19.6%.

Although widely scattered, band position appears to shift toward longer wavelengths with rising temperature [Fig. 11(c)]. All three data sets are somewhat erratic in band position throughout the temperature range. Combining the data yields a trend toward longer wavelengths as temperature increases. Because the band of data points in Fig. 11(c) is so wide, no attempt to fit a curve to the data was made.

Temperature-dependent behavior can be seen in bandwidth. With rising temperature, the spectral band broadens from 31 nm to 51.5 nm over the temperature range examined. Table 8 shows the increase to be apparent in all three data sets.

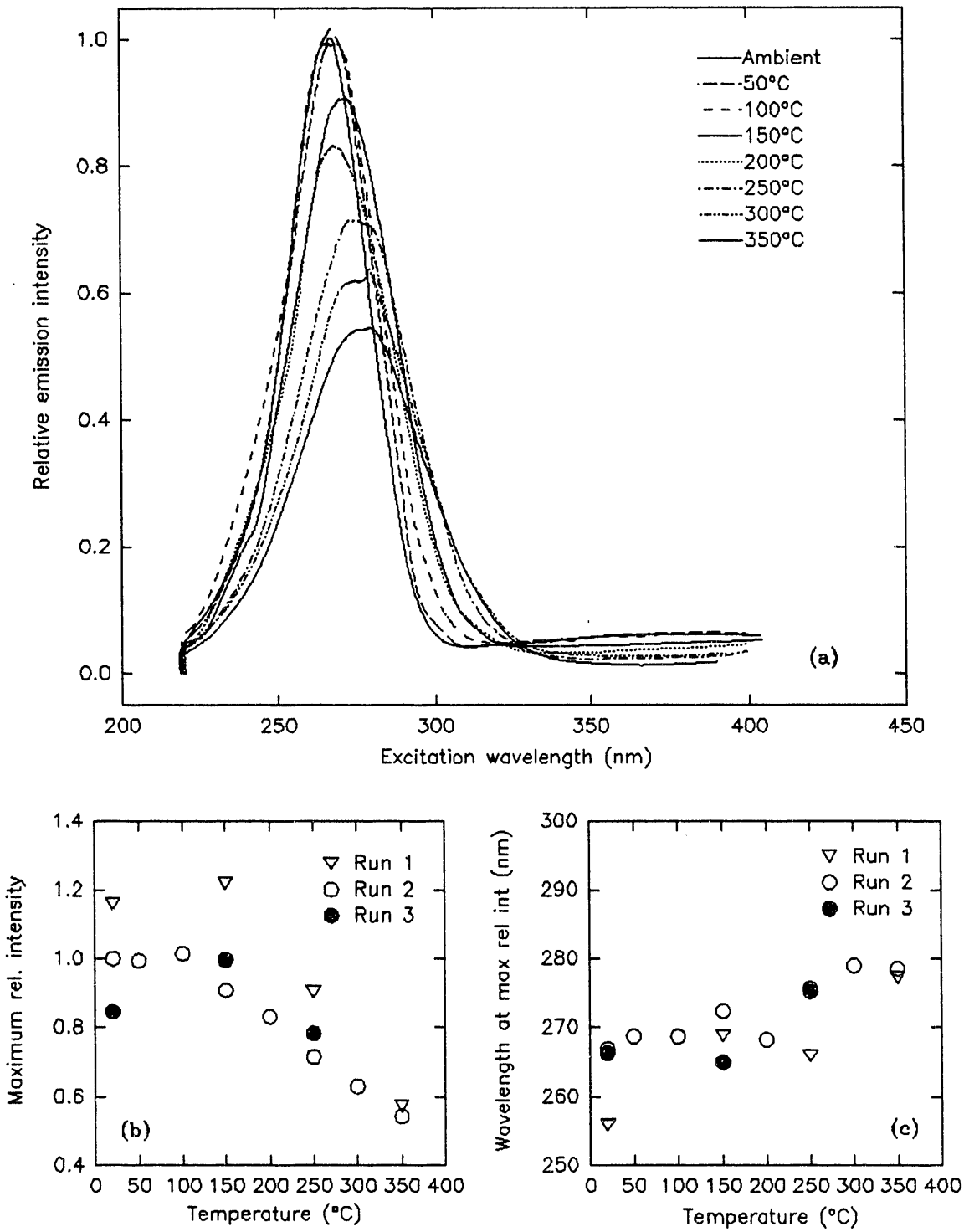

Fig. 11. Excitation data for $Sr_2P_2O_7$:Sn. (a) Excitation spectra, (b) maximum relative intensity vs temperature, (c) band position vs temperature.

Table 8. Bandwidth of $Sr_2P_2O_7$:Sn excitation as a function of temperature

	Bandwidth (nm)		
T(°C)	Run 1	Run 2	Run 3
amb	31	33	33
50	-	35	-
100	-	37.1	-
150	39.5	41.2	41.2
200	-	37.1	-
250	44	41.2	45.3
300	-	45.3	-
350	48	51.5	-

Many temperature-dependent trends are noted in this phosphor. Intensity is most sensitive to temperature in the range of 100°C to 350°C. Figure 10(a) implies entire quenching of the phosphor is well above 350°C. Higher-temperature study is not possible without a higher sensitivity PMT than in the present setup, because the emission signal over the entire range is weak. A band shift toward shorter wavelengths is apparent in emission data. A strong broadening of the excitation band is also evident.

4.5 $(BaMg)_3Si_2O_7$:Eu (Sylvania Type 217)

4.5.1 Emission

Emission spectra were obtained by exciting this sample with 370-nm light. An obvious temperature-dependent decrease in maximum relative intensity can be seen in Fig. 12(a). The collection of spectra show a sharp decrease in intensity from 100°C to 200°C with less rapid decreases occurring at extreme ends of the temperature range studied. A shift in spectral band is also apparent between 50°C and 100°C.

Figure 12(b) illustrates the relationship between maximum relative intensity and temperature. A strongly temperature-dependent intensity change occurs at temperatures from ambient to 250°C. At temperatures of 250°C and higher, the relative intensity is low and approaches zero in a much more gradual fashion. This suggests an exponential rather than a linear relationship.

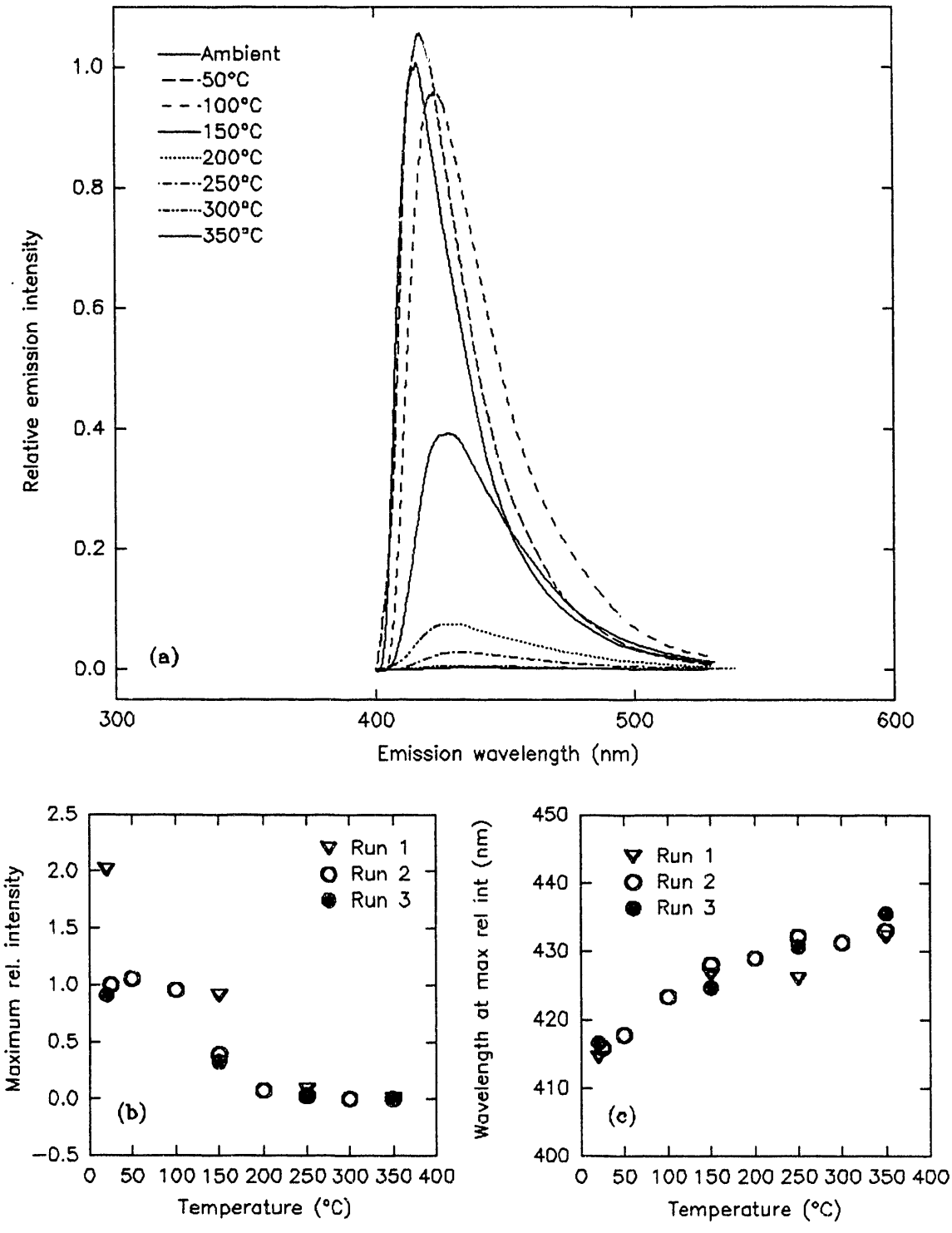

Fig. 12. Emission data for $(BaMg)_3Si_2O_7$:Eu. (a) Emission spectra, (b) maximum relative intensity vs temperature, (c) band position vs temperature.

Emission spectra maxima shift toward longer wavelengths as temperature increases. In Fig. 12(c), a strong linear dependence is suggested. All three data sets imply a direct relationship as temperature increases that can be mathematically stated

$$I_{max} = 5.3\text{x}10^{-2} \cdot T + 416.3 \; . \tag{9}$$

This implies a shift of 5.3 nm for every 100°C increase.

Emission spectra exhibit a consistent broadening of bandwidth as temperature increases. Table 9 shows an increase from about 29 nm to 50 nm through 250°C (bandwidth at higher temperatures could not be accurately measured due to extremely low maxima).

Table 9. Bandwidth $(BaMg)_3Si_2O_7$:Eu emission as a function of temperature

	Bandwith (nm)		
T(°C)	Run 1	Run 2	Run 3
amb	29	28.6	26.2
50	-	28.6	-
100	-	35.7	-
150	47	42.8	40.5
200	-	50	-
250	50	-	-

4.5.2 Excitation

Excitation spectra were found for emissions of 420-nm light. Temperature-dependent trends in intensity follow those of emission spectra. Figure 13(a) and (b) indicates a similar decrease with increasing temperature. A rapid decrease occurs through 250°C. Beyond this temperature, the phosphor emission appears to quench. Again, this implies an exponential relationship.

Excitation band shift appears to remain constant [Fig. 13(c)]. Data from Runs 2 and 3 indicate spectra intensities peak at approximately 372 nm regardless of phosphor temperature. Spectra from Run 1 have maxima occurring at lower wavelengths in the 330-nm range. These data fluctuate but show no particular trend toward higher or lower wavelengths. In light of data from Runs 2 and 3 with no decisive trend from Run 1, no temperature dependence is apparent for excitation spectra.

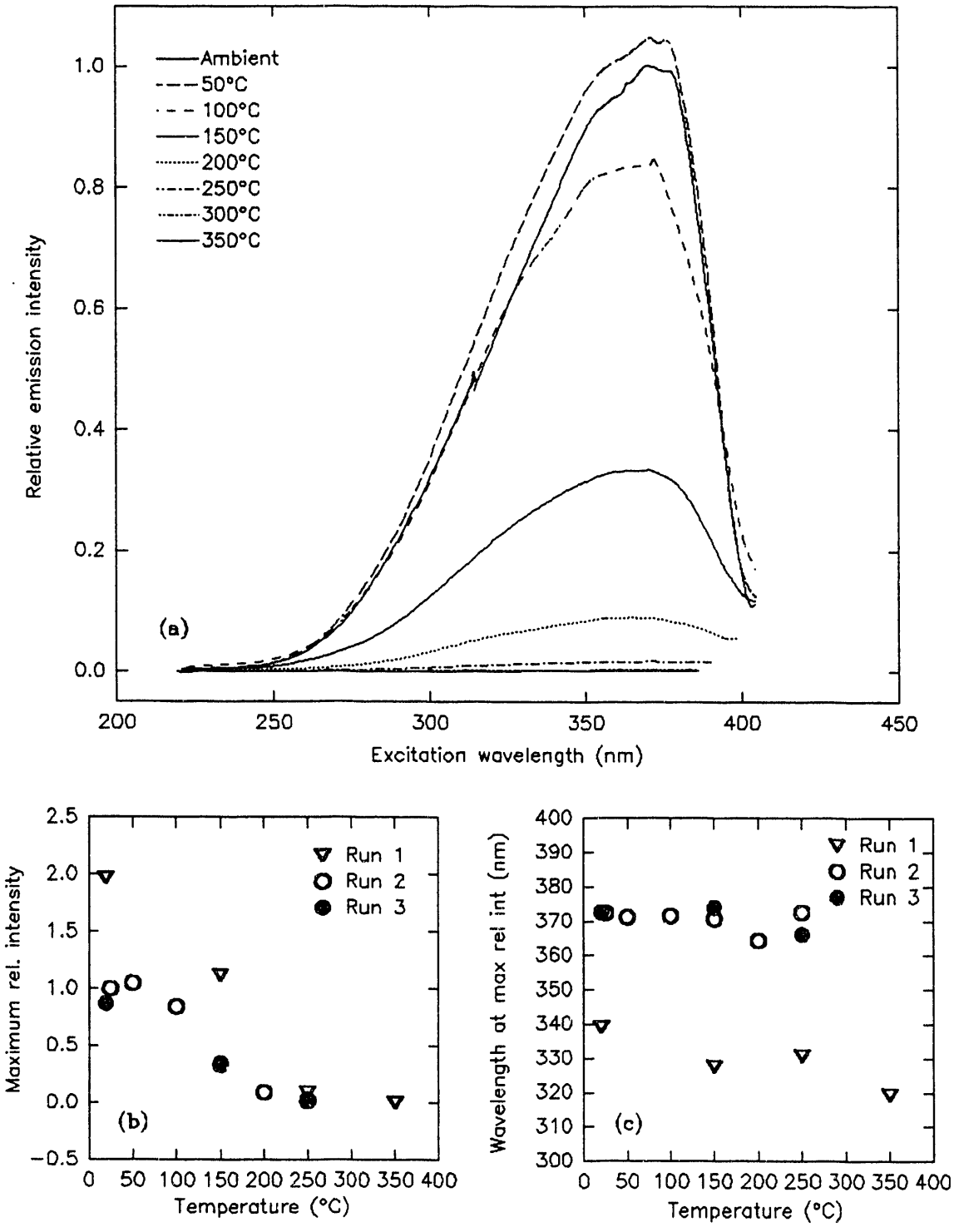

Fig. 13. Excitation data for $(BaMg)_3Si_2O_7$:Eu. (a) Excitation spectra, (b) maximum relative intensity vs temperature, (c) band position vs temperature.

Excitation spectra suggest the possibility for a broadening bandwidth (Table 10). Data from Run 2 suggests an increase in bandwidth; however, Run 1 does not support this finding and Run 3 offers only insufficient data, lending no credence to any trend.

Table 10. Bandwidt h of $(BaMg)_3Si_2O_7$:Eu excitation as a function of temperature

	Bandwidth (nm)		
T(°C)	Run 1	Run 2	Run 3
amb	111	76.8	80.9
50	-	80.1	-
100	-	85.1	-
150	106	91.3	85.1
200	-	-	-
250	106	-	-

Available data strongly support temperature-dependent trends for relative intensity and emission spectral shift and broadening. The broadening of emission bands is notably greater than temperature-dependent changes for many other phosphors studied in this experiment. Maximum relative intensity does approach zero at the high end of the temperature range indicating no probable applications above 350°C.

4.6 $Sr_2P_2O_7$:Eu (Sylvania Type 216)

4.6.1 Emission

A 352-nm excitation light was used to produce emission spectra from Fig. 14(a). The maximum relative intensity shows an increase from ambient to 50°C. A sharp decrease occurs from 100°C to 250°C and emission proceeds to decrease until it appears to quench at 350°C. The spectra exhibit no obvious band shift with changing temperature.

When comparing temperature directly with maximum relative intensity from Fig. 14(a) and two other data sets, a strong temperature-dependent trend emerges. Data from Run 2 provides the backbone for this trend, which is marked by a rapid decrease from 100°C to 200°C [see Fig. 14(b)]. This decrease, shown by all three data sets, indicates an 8.7% drop in relative intensity per 1°C increase in temperature. Temperatures beyond 200°C show a very gradual decrease in emission intensity, converging toward zero. The overall temperature-dependent trend appears to follow an exponential decrease.

The emission band does appear to shift toward longer wavelengths as temperature increases. As Fig. 14(c) illustrates, a slow linear trend can be seen with increasing temperature. This is best fit with the equation.

ORNL-DWG 92-12953

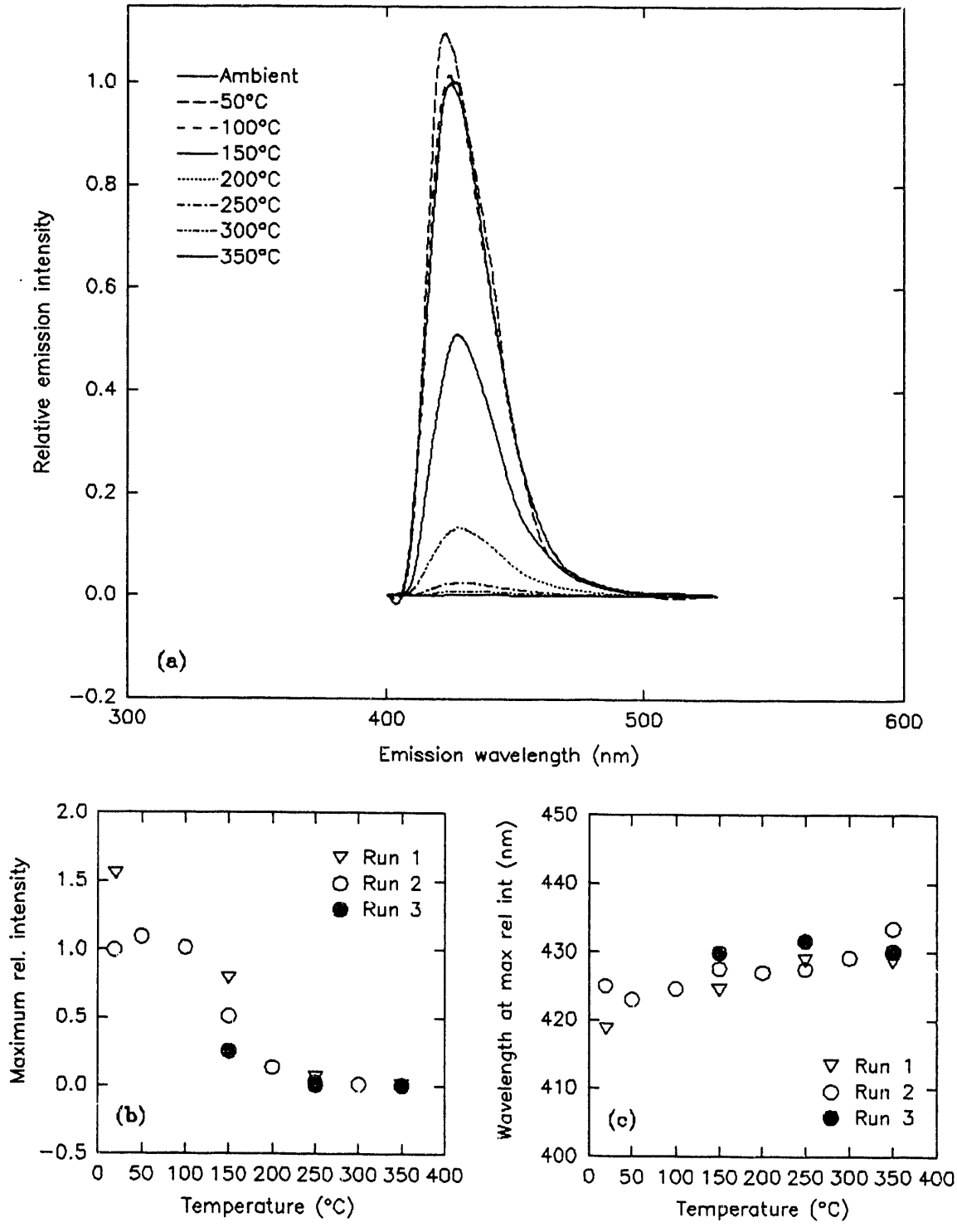

Fig. 14. Emission data for $Sr_2P_2O_7$:Eu. (a) Emission spectra, (b) maximum relative intensity vs temperature, (c) band position vs temperature.

$$I_{max} = 2.603\text{x}10^{-2} \cdot T + 422.2 \, . \qquad (10)$$

In short, the emission band shifts approximately 8.6 nm over the temperature range studied. This translates into approximately 2.6 nm for every 100°C increase. This is not a significantly large change to be applicable in phosphor-based thermometry.

Table 11 suggests that bandwidth for emission spectra remains constant. Insignificant increases of about 2 nm occur at temperatures around 150°C to 250°C.

Table 11. Bandwidth of $Sr_2P_2O_7$:Eu emission as a function of temperature

	Bandwidth (nm)		
T(°C)	Run 1	Run 2	Run 3
amb	26	27.3	-
50	-	27.3	-
100	-	27.3	-
150	28	27.3	29.5
200	-	29.6	-
250	32	-	-

4.6.2 Excitation

Excitation spectra for emissions of 428-nm light exhibit the same temperature-dependent trends emission spectra show. Figure 15(a) records a rise in relative intensity from ambient to 50°C and a sharp decrease from 100°C to 250°C. No obvious band shift is apparent.

Figure 15(b) illustrates the relationship between temperature and maximum relative intensity. Once again, the plot is noticeably marked by the rapid drop in intensity between 100°C and 200°C. This decrease implies that for every 1°C increase, intensity drops by 9.05%. Intensity continues to decrease as temperature rises, but at a significantly reduced rate. At 350°C, emissions seem to quench.

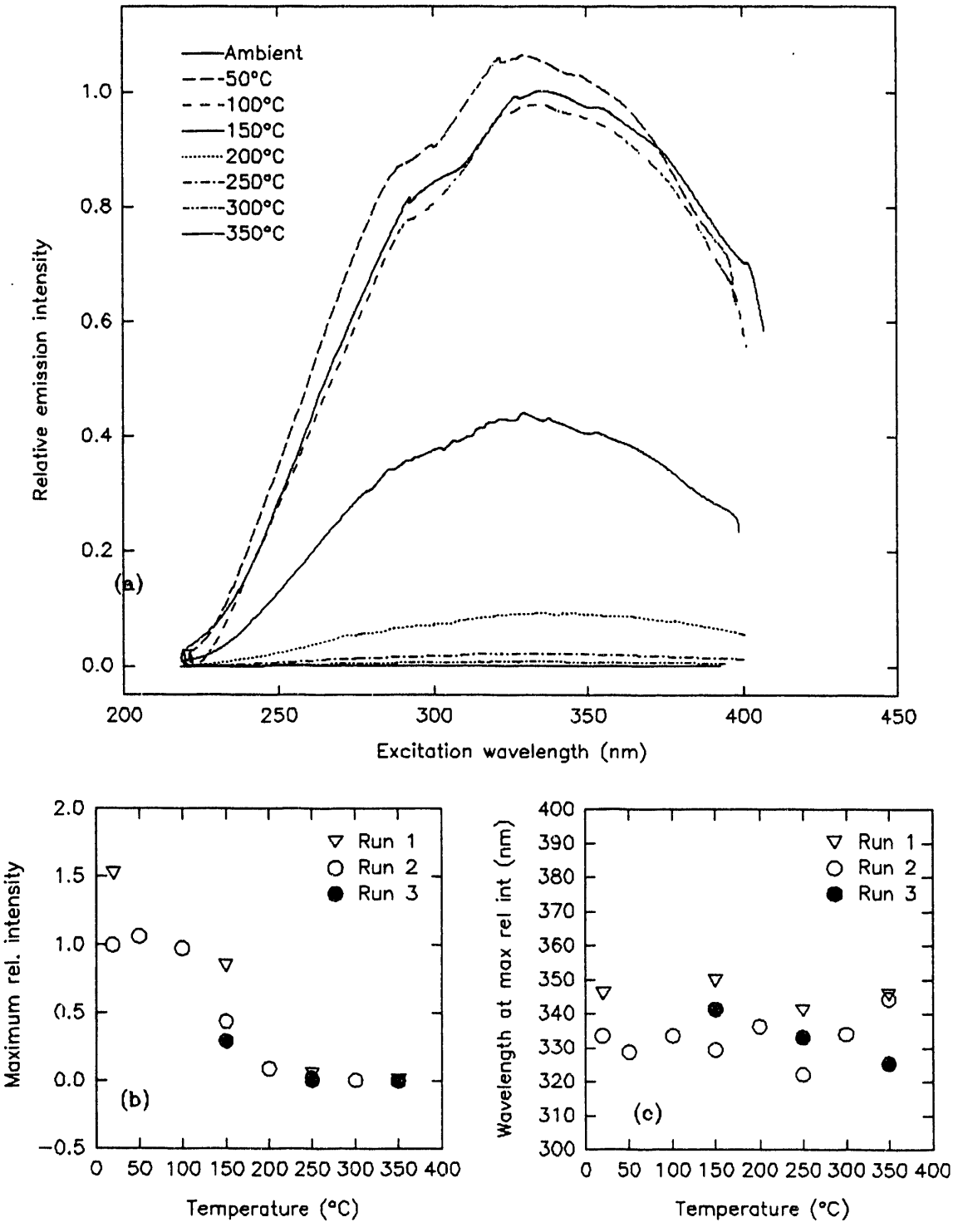

Fig. 15. Excitation data for $S_2P_2O_7$:Eu. (a) Excitation spectra, (b) maximum relative intensity vs temperature, (c) band position vs temperature.

Wavelengths at which maxima occur are scattered over a range of 325 to 350 nm [Fig. 15(c)]. Run 3 suggests band shifts to lower wavelengths. However, Runs 1 and 2, although widely scattered, do not support any uniform band shift to higher or lower wavelengths.

Bandwidths for data from Runs 2 and 3 remain constant at 138 nm (Table 12). Run 1 spectra have a narrower band that reduces 8 nm in width in a 230°C range. It cannot be determined if any temperature-dependent trend actually exists with the present data.

Table 12. Bandwidth $Sr_2P_2O_7$:Eu excitation as a function of temperature

	Bandwidth (nm)		
T(°C)	Run 1	Run 2	Run 3
amb	119	138	-
50	-	141.7	-
100	-	138	-
150	115	138	29.5
200	-	-	-
250	111	-	-
300	-	45.2	-
350	55.9	47.5	47.5

Strong temperature-dependent trends are found in maximum relative intensity for both emission and excitation spectra. The intensity also decreases to very low levels at the high end of the temperature range. This indicates little probable application for temperatures above 350°C. A small band shift toward longer wavelengths is also found in emission spectra.

4.7 $Ba_3(PO_4)_2$:Eu (Sylvania Type 215)

4.7.1 Emission

Spectra in Fig. 16(a) were taken when the phosphor sample was illuminated with 331 nm excitation light. Spectra shown on this graph increase in relative intensity from ambient to 50°C. A gradual decrease occurs from 50°C to 150°C. Temperatures below 150°C continue to decrease at an increasingly rapid rate. The band shifts toward higher wavelengths between 50°C and 100°C, but shows no significant shift elsewhere.

Delving further into the relationship between relative intensity and temperature, Fig. 16(b) plots data from all three runs against temperature. Each data set appears to decrease in a similar yet distinct manner. Runs 2 and 3 decrease in a near-identical exponential fashion. Run 2 is more

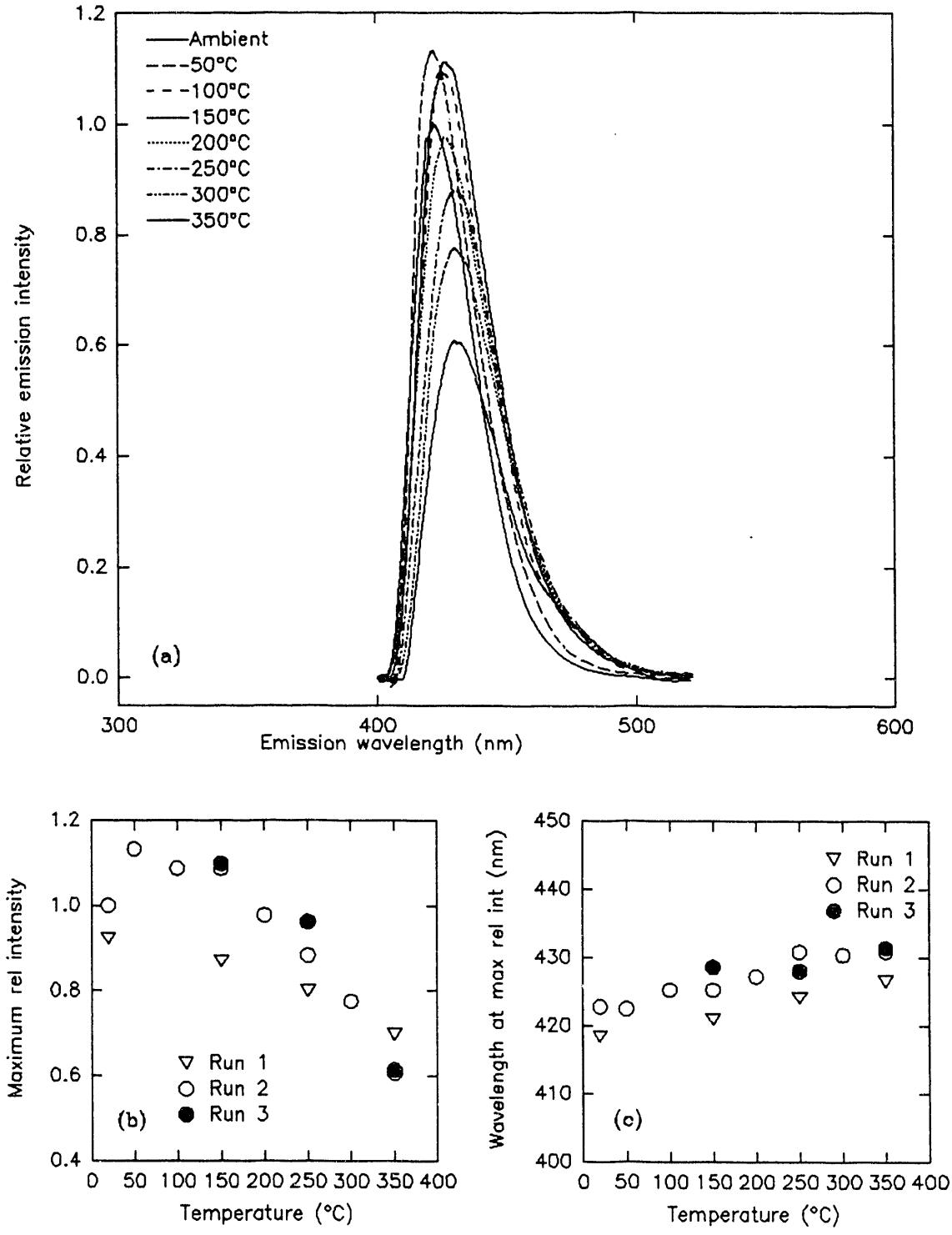

Fig. 16. Emission data for $Ba_3(PO_4)_2$:Eu. (a) Emission spectra, (b) maximum relative intensity vs temperature, (c) band position vs temperature.

detailed in the low range, showing an increase in the first temperature step followed by the exponential trend. Run 1 also shows a smooth exponential decrease as temperature increases. This data set does not detail trends between ambient and 150°C. Intensity decreases 47.4% over the entire temperature range.

A temperature-dependent band shift can be seen in Fig. 16(c). Data from Run 1 originates and shifts to slightly shorter wavelengths than the other two data sets, but does so at the same rate (i.e., has the same slope). The equation describing the data is

$$I_{max} = 2.665\text{x}10^{-2} \cdot T + 421 \; . \tag{11}$$

This implies a 2.7 nm shift every 100°C, which does not provide much sensitivity for temperature detection.

No significant broadening of the spectral band is exhibited for this sample. Table 13 shows constant bandwidth throughout the temperature range with the exception of a small jump between 150°C and 200°C for Runs 2 and 3. Run 1 indicates a small increase in bandwidth throughout the temperature range. However, the increase is only 2 nm for every 100°C which is of marginal significance.

Table 13. Bandwidth of $Ba_3(PO_4)_2$:Eu emission as a function of temperature

	Bandwidth (nm)		
T(°C)	Run 1	Run 2	Run 3
amb	28.2	27.3	-
50	-	27.3	-
100	-	27.3	-
150	30.4	27.3	31.9
200	-	31.9	-
250	32.6	31.9	31.9
300	-	31.9	-
350	34.8	31.9	31.9

4.7.2 Excitation

Excitation spectra for emission of 425-nm light are recorded in Fig. 17(a). The excitation spectra are similar to the emission spectra in that the relative intensity increases with temperature in the low range and decreases rapidly in the mid to high range studied. However, the excitation intensity is shown to increase through 100°C (increase occurred through 50°C for emission spectra). No trend in band shift is obvious in the collection of spectra.

Looking more closely at temperature dependence found in relative intensity reveals trends similar to those found for emission spectra [Fig. 17(b)]. Once again, a curve of rapid decrease for temperatures above 100°C appears to be smooth and relatively predictable. Data from Run 2 also indicate an increase in intensity at the low end of the temperature range, ambient through 100°C.

Figure 17(c) depicts the relationship between spectral band shift and temperature. A suggestion of gradual movement toward longer wavelengths is indicated. The shift is similar to the emission spectra in that movements toward longer wavelengths of approximately 8 nm occurred over the entire temperature range.

Bandwidth was noted to broaden 16 nm from ambient to 350°C. Table 14 lists the bandwidths, showing a clear increase with temperature for Runs 1 and 2.

Table 14. Bandwidth of $Ba_3(PO_4)_2$:Eu excitation as a function of temperature

	Bandwidth (nm)		
T(°C)	Run 1	Run 2	Run 3
amb	89	90.9	
50	-	95	-
100	-	97.1	-
150	96	99.1	99.1
200	-	99.1	-
250	104	103	107
300	-	103	-
350	104	107	103

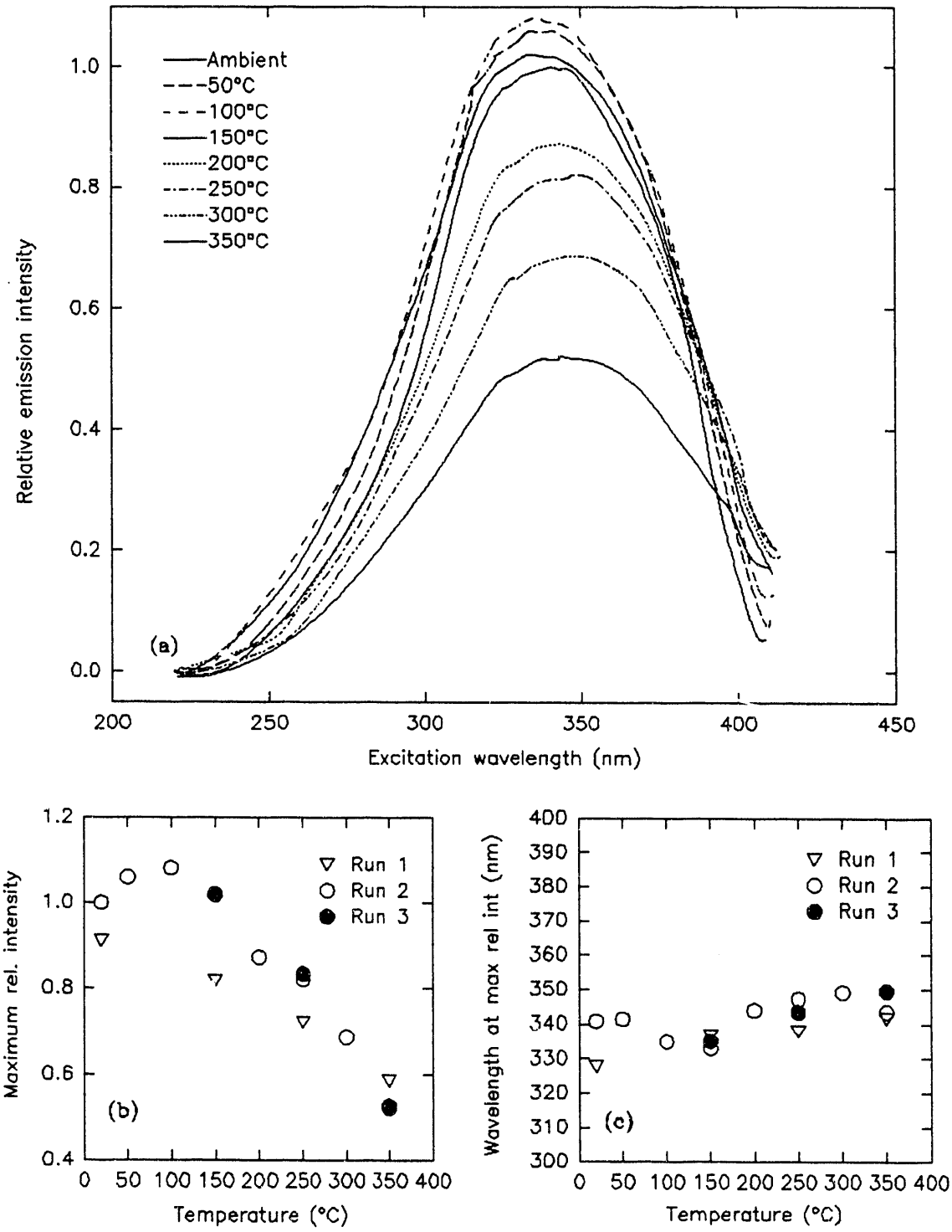

Fig. 17. Excitation data for $Ba_3(PO_4)_2$:Eu. (a) Excitation spectra, (b) maximum relative intensity vs temperature, (c) band position vs temperature.

A unique characteristic of this phosphor over others examined in this study is the level of intensity at 350°C. Unlike other samples, the relative intensity is well above zero and the point of entire quenching of emissions at the high end of the temperature range. It has a high unnormalized relative intensity that the PMT can easily detect at 350°C and, as Fig. 16(a) shows, has only decreased in intensity a total of about 60% (other phosphors studied show decreases of 90% and above). Continuing study through higher temperatures may lead to findings useful for high-temperature applications.

A spectral shift is also notable in both emission and excitation spectra. Because the shift occurs at a gradual rate, band shift will probably not provide the degree of sensitivity required for thermographic applications. However, the change should be noted for cases in which that shift may interfere with other spectral readings.

4.8 Y_2SiO_5:Ce (Sylvania Type 158)

4.8.1 Emission

This phosphor, when excited by 358-nm light, produces spectra that rapidly fall off in intensity. Figure 18(a) shows the spectra. The range that appears to have the greatest decrease is from 50°C to 200°C. Spectra below 200°C approach zero intensity and indicate quenching of the phosphor.

Figure 18(b) plots maximum relative intensity against temperature. As previously seen, a sharp decrease with rising temperature occurs through 200°C. Through this range, intensity is dropping off at a rate of 43.4% per 100°C. Higher temperatures show intensity gradually approaching zero.

A shift toward longer wavelengths, from 431 nm to 435 nm, is indicated by data from Runs 2 and 3. Most of the shifting occurs at temperatures above 100°C. Run 1 implies a more constant band position at overall shorter wavelengths (425 nm to 429 nm). Conflicting data make good predictions of temperature-dependent behavior difficult.

Bandwidth was only measured for spectra at 250°C and below (spectral intensities for higher temperatures were too small for bandwidth measurement). For this range, no temperature-dependent behavior was observed. Table 15 lists stable bandwidths at about 50 nm.

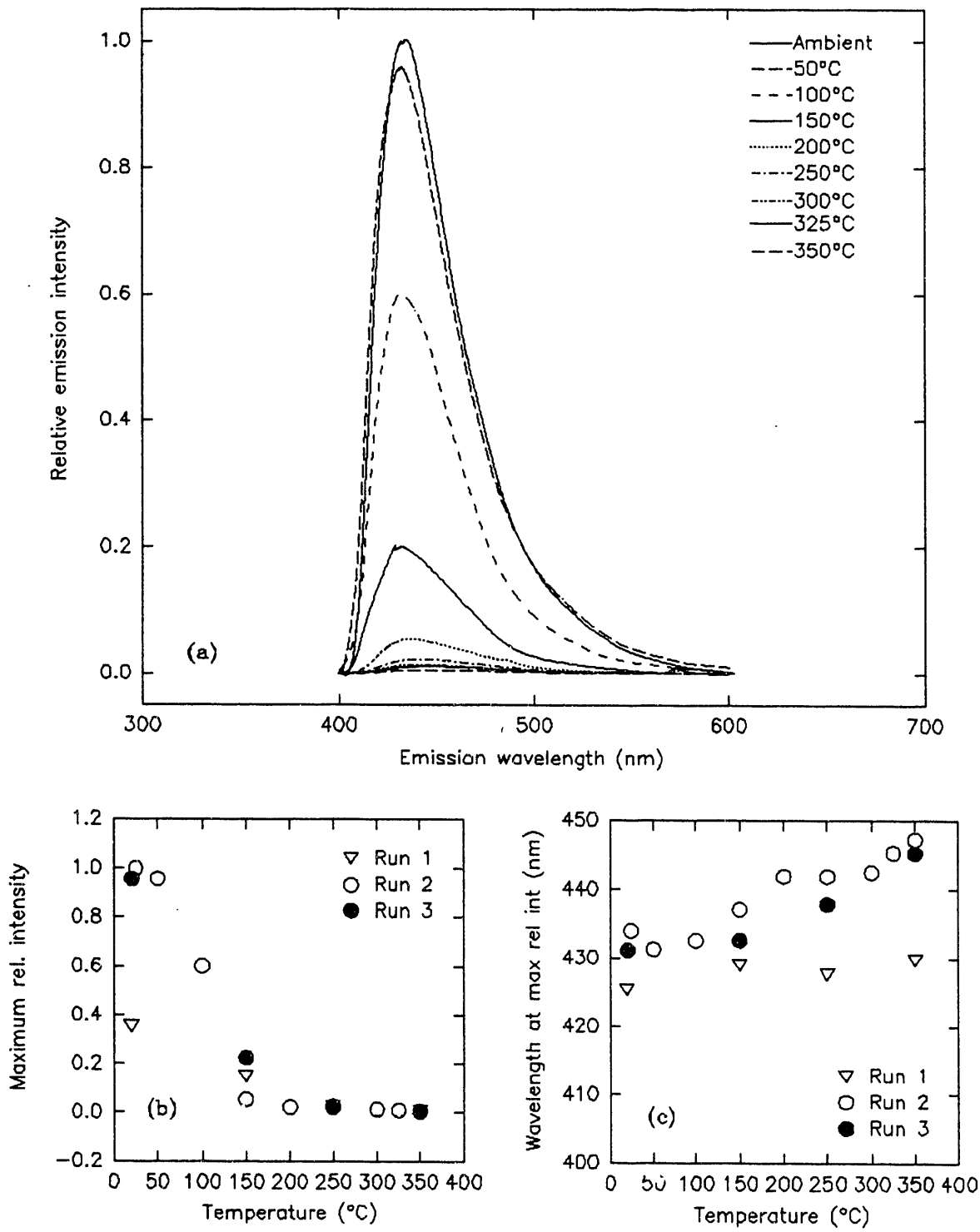

Fig. 18. Emission data for Y_2SiO_5:Ce. (a) Emission spectra, (b) maximum relative intensity vs temperature, (c) band position vs temperature.

Table 15. Bandwidth of Y_2SiO_5:Ce emission as a function of temperature

	Bandwidth (nm)		
T(°C)	Run 1	Run 2	
amb	48.5	50	51.3
50	-	52.6	-
100	-	51.3	-
150	48.5	55.9	52.6
200	-	-	-
250	48.5	-	-

4.8.2 Excitation

Excitation spectra taken for 433-nm emissions is shown in Fig. 19(a). In addition to the maxima, a secondary hump occurs centering around 320 nm and fading at 300°C. Both peaks decrease rapidly in the range from 50°C to 200°C, approaching zero relative intensity above this range.

The rapid decrease in relative intensity is evident in Fig. 19(b). The slope of a line fit to the range of ambient to 200°C implies a 51.6% decrease for 100°C increments. This behavior is similar to that of emission spectra.

Spectral band position appears to shift toward shorter wavelengths at very low relative intensities. At temperatures of 200°C to 350°C, a band shift from 360 nm to 345 nm occurs.

Bandwidth also appears to have temperature-dependent qualities. All data sets indicate that the spectral band is widening from about 32 nm in width at ambient to approximately 46 nm at 250°C. These measurements can be found in Table 16.

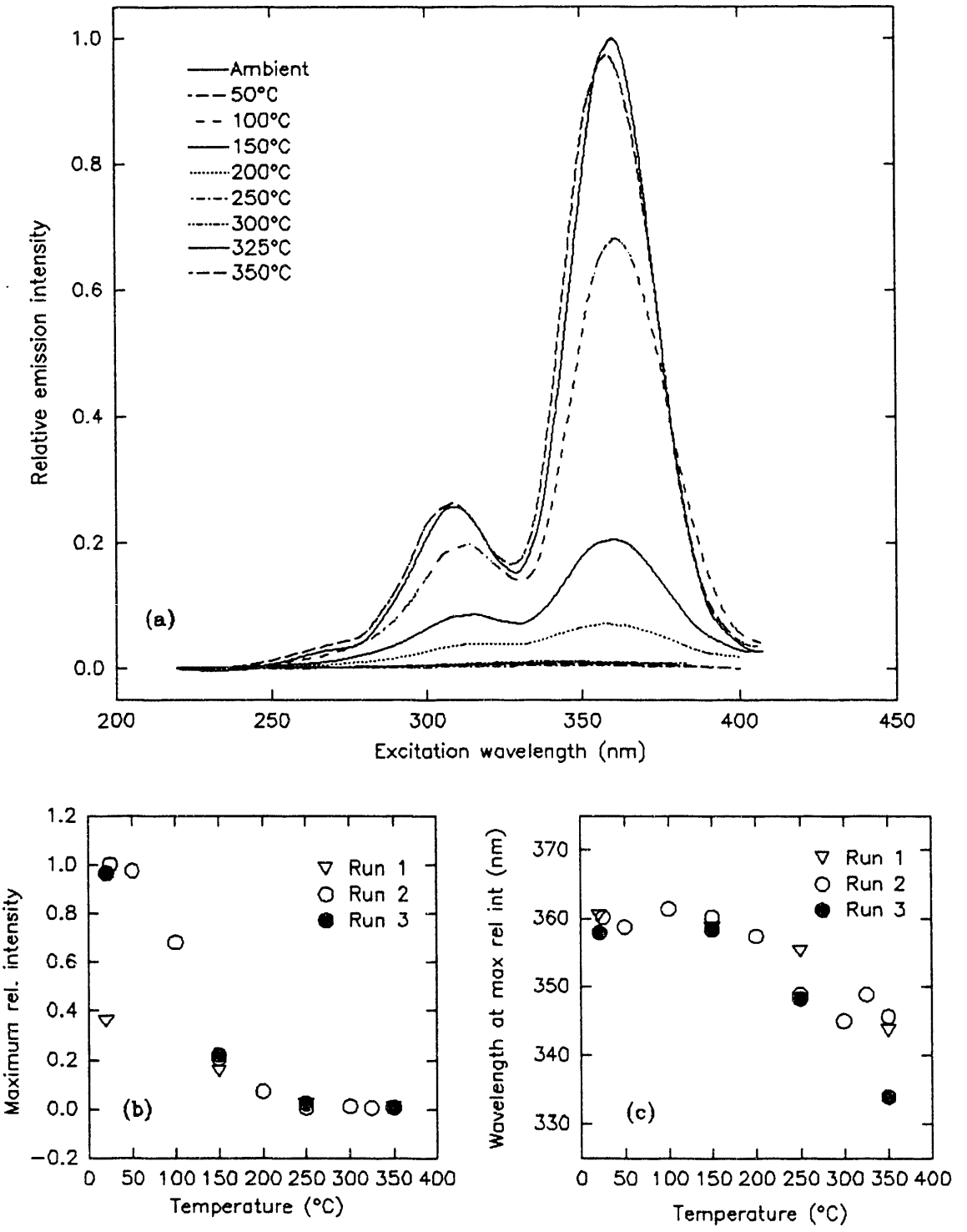

Fig. 19. Excitation data for Y_2SiO_5:Ce. (a) Excitation spectra, (b) maximum relative intensity vs temperature, (c) band position vs temperature.

Table 16. Bandwidth of Y_2SiO_5:Ce excitation as a function of temperature

	Bandwidth (nm)		
T(°C)	Run 1	Run 2	Run 3
amb	32	33	39.2
50	-	33	-
100	-	37.2	-
150	38	42.3	41.3
200	-	-	-
250	46	-	

Emission and excitation spectra share similar temperature-dependent behavior for decrease in relative intensity. The sharp change in intensity from 50°C to 200°C distinctly marks this phosphor. Band shift and band broadening also occur in excitation spectra at high temperatures in the range studied. However, emissions also are nearly zero at these temperatures, severely limiting use of these temperature-dependent properties.

5. CONCLUSION

Phosphors in this study all show temperature dependence in their emission spectra. In all cases, emission intensities decreased with increasing temperature. Five of the eight phosphors, $Ca_5F(PO_4)_3$:Sb, $Sr_5Cl(PO_4)_3$:Eu, $(BaMg)_3Si_2O_7$:Eu, $Sr_2P_2O_7$:Eu, and Y_2SiO_5:Ce, appear to nearly or entirely quench by 350°C.

$BaMg_2Al_{16}O_2$:Eu and $Ba_3(PO_4)_2$:Eu show promise for higher-temperature studies. Both have strong unnormalized intensities at the high end of the temperature range for this experiment and do not appear to quench in normalized spectra presented in the results. $Sr_2P_2O_7$:Sn also appears to be a candidate for high-temperature studies; however, the intensity of the emissions for this phosphor was initially weak at ambient temperatures. Limitations of the PMT restrict further study of this phosphor.

Strong band shifts were noted in $Sr_2P_2O_7$:Sn and $(BaMg)_3Si_2O_7$:Eu emission spectra. As temperature increased from 20°C to 350°C, $Sr_2P_2O_7$:Sn shifted 4.4 nm toward shorter wavelengths and $(BaMg)_3Si_2O_7$:Eu moves 5.3 nm toward longer wavelengths. Other phosphors either showed no temperature dependence related to band position, erratic jumps in band position, or only a very slight change.

Broadening of spectral bands was found to be significant in $(BaMg)_3Si_2O_7$:Eu and $Sr_5Cl(PO_4)_3$:Eu emission spectra. The emission data for the other phosphors indicated no increase in bandwidths with varied temperature.

It should also be noted that several phosphors showed inconsistencies in trends at ambient to 100°C. Data sets for these phosphors conflicted, indicating a strong decreasing trend for one set and an increasing trend at low temperatures (peaking in the range 50°C to 100°C) and then a decreasing trend (similar to the other data set). The incongruity is thought to be due to the spectrophotometer. It has been observed that the relative intensity of the spectrophotometer rises and does not stabilize for 30 min after initial operation. Many of the readings at ambient and 50°C temperatures were taken during this period.

This evaluation leads to the conclusion that emission intensities are the most strongly and easily identifiable temperature-dependent properties in the phosphors studied. For applications in phosphor thermometry, these samples show linear and exponential dependencies with temperature. These dependencies are easy to model and can, therefore, be more easily used in applications. The phosphors which show no temperature dependence in bandwidth and band position also are better for intensity-based applications.

Another distinguishing characteristic of these phosphors is their blue emission. An obvious application would be to find the proper combination of phosphors of different color emissions to identify a large temperature region. Blue phosphors from this study could be applicable in such a situation. A disadvantage of the particular samples studied in this experiment is their large bandwidth. Blue-emitting phosphors with sharper peaks would be less likely to interfere or overlap with emissions from other phosphors.

Blue-emitting phosphors also offer better readings where blackbody radiation produces interference. Blackbody radiation has less blue radiance than other longer-wavelength light. For example, at 1200°C, red emittance from blackbody radiation is two orders of magnitude higher than blue. Thus, a red-emitting phosphor would not fair as well as a blue-emitting phosphor where blackbody radiation is present. In the case in which a cool surface must be measured in the midst of a very hot region (where blackbody radiation is high), blue phosphors such as the ones studied for this experiment would be ideal.

These are just a few applications possible for these phosphors. As applications and their subsequent requirements arise, this study can offer basic information on the thermographic properties of these phosphors for temperatures through 350°C. Emission lifetimes would be another temperature-dependent characteristic to study in future work. High-temperature studies may also yield further uses for some of the samples studied.

ACKNOWLEDGMENTS

The authors thank Helen S. Payne and the Science and Engineering Semester (SERS) Program for supporting Debra Cunningham during the term of this research project. The SERS Program is funded by the DOE Office of Energy Research National Program and is administered by the ORNL University Programs Office.

BIBLIOGRAPHY

S. W. Allison et al., *Solid-State Fluorescence Above 1000°C: Application to High-Temperature Laser Thermometry,* Report No. ORNL/ATD-21, Martin Marietta Energy Systems, Inc., Oak Ridge, TN, January 1990.

A. R. Bugos, *Characterization of the Emission Properties of Thermographic Phosphors for Use in High Temperature Sensing Applications,* Master's Thesis, University of Tennessee, Knoxville, May 1989.

K. H. Butler, *Fluorescent Lamp Phosphors,* The Pennsylvania State University Press, University Park, PA, 1980.

R. G. Hellier, *Development of Temperature Imaging Techniques Using Thermographic Phosphors,* Master's Thesis, University of Virginia, Charlottesville, January 1992.

INTERNAL DISTRIBUTION

D. J. Adams
S. W. Allison (10)
D. L. Beshears
M. R. Cates
J. E. Jones Jr.
W. S. Key
D. N. Mashburn
S. A. McElhaney
W. C. McWhorter
J. D. Muhs
M. A. Simpson
D. B. Smith (5)
Laboratory Records-RC (3)

DEPARTMENT OF ENERGY FIELD OFFICE, OAK RIDGE

Assistant Manager, Energy Research and Development

EXTERNAL DISTRIBUTION

Debra M. Cunningham, Swarthmore College, Swarthmore, PA
G. T. Gillies, University of Virginia, Dept. of Nuclear Engineering and Engineering Physics
B. W. Noel, Los Alamos National Laboratory, Los Alamos, NM
H. Payne, Office of University and Education Programs
D. Turley, EG&G Energy Measurements, Goleta, CA
Office of Scientific and Technical Information (2), P.O. Box 62, Oak Ridge, TN 37831

END

DATE FILMED

6 / 11 / 93